



OPEN

## Intragastric administration of short chain fatty acids greatly reduces voluntary ethanol intake in rats

**Maria Elena Quintanilla**<sup>1,2,11</sup>, **Daniela Santapau**<sup>3,11</sup>, **Eugenio Diaz**<sup>4</sup>,  
**Ignacio Valenzuela Martinez**<sup>5</sup>, **Nicolas Medina**<sup>5</sup>, **Glauben Landskron**<sup>6</sup>, **Antonia Dominguez**<sup>6</sup>,  
**Paola Morales**<sup>1,2,4,7</sup>, **David Ramirez**<sup>5,7</sup>, **Marcela Hermoso**<sup>8,9</sup>, **Belén Olivares**<sup>10</sup>,  
**Pablo Berrios-Cárcamo**<sup>3</sup>, **Marcelo Ezquer**<sup>3</sup>, **Mario Herrera-Marschitz**<sup>4</sup>, **Yedy Israel**<sup>1,2</sup> &  
**Fernando Ezquer**<sup>3,7✉</sup>

Alcohol use disorder (AUD) represents a public health crisis with few FDA-approved medications for its treatment. Growing evidence supports the key role of the bidirectional communication between the gut microbiota and the central nervous system (CNS) during the initiation and progression of alcohol use disorder. Among the different protective molecules that could mediate this communication, short chain fatty acids (SCFAs) have emerged as attractive candidates, since these gut microbiota-derived molecules have multi-target effects that could normalize several of the functional and structural parameters altered by chronic alcohol abuse. The present study, conducted in male alcohol-preferring UChB rats, shows that the initiation of voluntary ethanol intake was inhibited in 85% by the intragastric administration of a combination of SCFAs (acetate, propionate and butyrate) given before ethanol exposure, while SCFAs administration after two months of ethanol intake induced a 90% reduction in its consumption. These SCFAs therapeutic effects were associated with (1) a significant reduction of ethanol-induced intestinal inflammation and damage; (2) reduction of plasma lipopolysaccharide levels and hepatic inflammation; (3) reduction of ethanol-induced astrocyte and microglia activation; and (4) attenuation of the ethanol-induced gene expression changes within the nucleus accumbens. Finally, we determined that among the different SCFAs evaluated, butyrate was the most potent, reducing chronic ethanol intake in a dose-response manner. These findings support a key role of SCFAs, and especially butyrate, in regulating AUD, providing a simple, inexpensive, and safe approach as a preventive and intervention-based strategy to address this devastating disease.

**Keywords** Alcohol abuse, Gut microbiota-brain axis, SCFAs, Butyrate, Alcohol use disorder treatment

Alcohol is the most consumed addictive substance in the world, often leading to the development of alcohol use disorders (AUD)<sup>1</sup>. Alcohol dependence has traditionally been considered a brain disorder involving the alteration of various neurotransmitters and their receptors in specific areas such as the brain reward circuit<sup>2</sup>. These alterations play a major role in the positive and negative reinforcement processes driving the motivation for ethanol seeking<sup>2</sup>. However, pharmacological approaches targeting these neurotransmitter systems have generated only small therapeutic effects<sup>3</sup>, suggesting the involvement of other biological processes that could also be driving the addictive behavior.

<sup>1</sup>Molecular and Clinical Pharmacology Program, Institute of Biomedical Sciences, Faculty of Medicine, Universidad de Chile, Santiago, Chile. <sup>2</sup>Specialized Center for the Prevention of Substance Use and the Treatment of Addictions (CESA), Faculty of Medicine, Universidad de Chile, Santiago, Chile. <sup>3</sup>Center for Regenerative Medicine, Faculty of Medicine Clínica Alemana-Universidad del Desarrollo, Avenida Plaza 680, Santiago, Chile. <sup>4</sup>Department of Neuroscience, Faculty of Medicine, Universidad de Chile, Santiago, Chile. <sup>5</sup>Departamento de Farmacología, Facultad de Ciencias Biológicas, Universidad de Concepción, Concepción, Chile. <sup>6</sup>Center for Biomedical Research, CIBMED, Faculty of Medicine, Universidad Finis Terrae, Santiago, Chile. <sup>7</sup>Research Center for the Development of Novel Therapeutics Alternatives for Alcohol Use Disorders, Santiago, Chile. <sup>8</sup>Department of Gastroenterology and Hepatology, University Medical Center, Groningen, The Netherlands. <sup>9</sup>Laboratorio de Inmunidad Innata, Programa Disciplinario de Inmunología, ICBM, Facultad de Medicina, Universidad de Chile, Santiago, Chile. <sup>10</sup>Center for Medical Chemistry, Faculty of Medicine Clínica Alemana-Universidad del Desarrollo, Santiago, Chile. <sup>11</sup>These authors contributed equally to this work. ✉email: eezquer@udd.cl

Over the past few years, several studies have supported the role of the gut microbiota, a large community of microorganisms colonizing the intestine, as an important component mediating the development of neuropsychiatric disorders<sup>4</sup>, including addictive behaviors<sup>5,6</sup>. Alterations in gut microbiota composition, have been observed both in male and female patients presenting AUD<sup>7,8</sup> and in animal models characterized by high alcohol intake<sup>9,10</sup>. This disturbance in bacterial community could communicate with the central nervous system (CNS) through the gut brain axis, influencing brain function and behavior, thus accelerating the cycle of addiction<sup>5,9,11</sup>.

In animal models exposed to alcohol<sup>12,13</sup> and in alcohol-dependent individuals<sup>14,15</sup>, it has been reported that alcohol and its first metabolite, acetaldehyde, induce intestinal damage and inflammation, altering the intestinal epithelial permeability, a phenomenon known as “leaky gut”<sup>8</sup>. This hyper-permeable gut mucosa allows lipopolysaccharides (LPS) and other pro-inflammatory/pathogenic microbial products to easily reach the systemic circulation and activate the Toll-like receptor 4 (TLR4) of immune cells in target organs, including the liver and other peripheral tissues. Remarkably, microglia and astrocytes, the main immunological cells in the brain, also express TLR4 and consequently respond to pathogen-associated molecular patterns by producing pro-inflammatory cytokines<sup>16</sup>. This inflammatory response promotes neuroinflammation and epigenetic changes<sup>17</sup>, reducing glutamate transport<sup>18</sup>, thereby increasing extracellular glutamate levels that potentiate drinking behavior<sup>19,20</sup>. Conclusively, the use of TLR4-knockout mice demonstrates that activation of TLR4 in astrocytes and microglia following ethanol exposure is crucial for inducing neuroinflammation<sup>21</sup>. Moreover, intraperitoneal injection of LPS induces a long-lasting increase in ethanol intake in mice<sup>22</sup>, indicating a major role of increased gut permeability in alcohol addictive behavior.

A decrease in beneficial bacteria such as *Lactobacillus* and *Bifidobacterium* has been shown in animals exposed to alcohol and in alcohol-dependent patients<sup>9,15</sup>; therefore, restoring these anti-inflammatory bacteria could represent a potential therapeutic approach for improving alcohol-related diseases and reduce alcohol dependence. Accordingly, in animal models of alcohol-induced liver disease, modulation of the gut microbiota by *Lactobacillus GG* supplementation reduces gut leakiness, endotoxemia, and liver inflammation<sup>13</sup>. Moreover, *Lactobacillus GG* supplementation also reduces both (1) the acquisition of high ethanol intake when administered before ethanol exposure to the ethanol-drinking UChB rat strain<sup>5</sup> and (2) ethanol relapse when administered to chronically ethanol-drinking UChB animals<sup>9</sup>. Similarly, six months of *Lactobacillus GG* supplementation to alcohol-dependent patients attenuates liver injury and reduces heavy alcohol intake<sup>23</sup>, indicating that probiotic supplementation could be a therapeutic alternative for AUD treatment.

The mechanisms underlying the communication between the administered probiotics and the CNS mediating the behavioral effects have not yet been elucidated. However, the three main short-chain fatty acids (SCFAs; acetate, propionate, and butyrate), beneficial lipid metabolites generated by colonic dietary fiber fermentation by some anti-inflammatory gut bacterial strains<sup>24</sup>, have gained attention due to their anti-inflammatory properties and the ability to improve intestinal barrier integrity<sup>25,26</sup>. Additionally, SCFAs have neuroactive properties due to their role as histone deacetylase (HDAC) inhibitors<sup>27</sup>, directly influencing brain function and behavior<sup>28–30</sup>. Interestingly, alcohol consumption directly decreases the abundance of SCFA-producing bacteria<sup>15</sup> and lowers SCFA levels in stools and blood<sup>7,31</sup>. Thus, oral SCFA supplementation could represent an attractive alternative for the treatment of alcohol use disorder.

SCFAs supplementation has several advantages compared with the administration of probiotics, including (1) direct and rapid effects; (2) dosage consistency; (3) independence from interindividual microbiota variability, and (4) lower risk of infections and adverse effects<sup>32</sup>. Thus, in this work, we evaluated whether the intragastric administration of the SCFAs acetate, propionate and butyrate given before or after ethanol exposure prevent the acquisition phase of ethanol intake or reduce a previously established chronic alcohol consumption, respectively. We also explored the mechanism behind the SCFAs therapeutic effects by evaluating intestinal architecture and inflammation, liver inflammation, microglial and astrocyte activation, and transcriptional dynamics in the nucleus accumbens, the main brain center controlling drug addiction. Finally, we determined the most potent SCFA in reducing chronic ethanol intake and its effects on the levels of histone acetylation.

## Results

### Intragastric co-administration of SCFAs prevents the acquisition of high voluntary alcohol intake in ethanol-naïve rats

To determine whether the intragastric administration of SCFAs prevents the acquisition of ethanol intake, ethanol-naïve male UChB rats were given a combination of three SCFAs containing 300 mg/kg sodium acetate, 300 mg/kg sodium propionate and 300 mg/kg sodium butyrate dissolved in distilled water. A second group (control) was treated with 544 mg/kg of NaCl to rule out the influence of sodium provided by the three SCFAs on the intake of ethanol solution and water in the SCFAs treated group. Another control group received the vehicle (distilled water). All treatments were administered via oral gavage twice-daily for six days before access to ethanol.

Voluntary alcohol preference was subsequently evaluated daily for seven days while maintaining the two daily administrations of SCFAs or vehicle. Animals were offered a two-bottle-choice access between a 10% ethanol solution (v/v) and water. Data indicated that SCFAs administration induced an 85% reduction ( $p < 0.0001$ ) in voluntary ethanol intake (Fig. 1A) and in ethanol preference ( $p < 0.0001$ ) (Fig. 1B) compared with control animals treated with NaCl or the vehicle. The inhibition in alcohol intake induced by the SCFAs administration was fully compensated by an increase in water intake ( $p < 0.0001$ ) (Fig. 1C), normalizing the animal's hydric homeostasis (Fig. 1D). The finding that no increase in water intake was observed in control rats treated with NaCl rules out a possible role of the sodium provided by SCFAs in the increase in water intake observed in the SCFAs-treated group (Fig. 1C). Additionally, the finding that SCFAs administration did not induce changes in total fluid intake or body weight (Fig. 1D; top and bottom, respectively) compared with the NaCl- and vehicle-treated groups

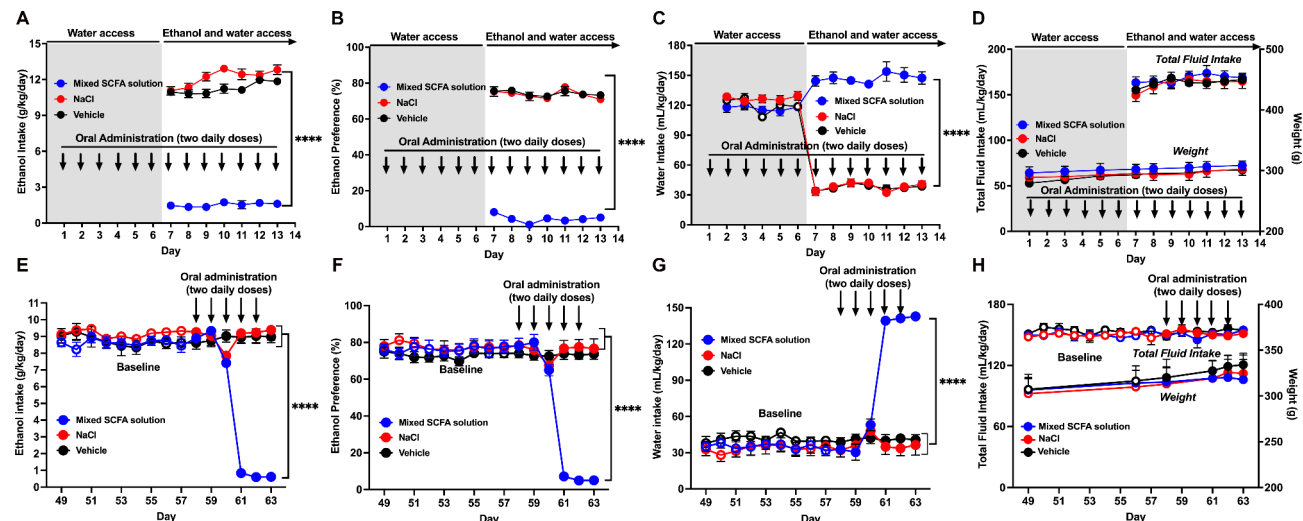


**Fig. 1.** Intragastric administration of SCFAs prevents voluntary alcohol intake and alcohol preference in ethanol-naïve animals and reduces voluntary alcohol intake and preference in animals chronically drinking ethanol. Ethanol-naïve male UChB rats were treated with either (1) a combination of SCFAs (300 mg/kg each sodium acetate, sodium propionate, and sodium butyrate), 554 mg/kg NaCl solution, or vehicle, by oral gavage twice-daily for six days. Next, animals were exposed to 10% ethanol solution and water. SCFAs or vehicle administration was maintained for additional seven days. (A) Voluntary ethanol intake is expressed in gr/kg body weight/day. We observed a significant effect of treatment [ $F_{\text{treatment}(2,15)} = 662.1, p < 0.0001$ ], day [ $F_{\text{day}(3613, 54.19)} = 10.88, p < 0.0001$ ] and a significant treatment  $\times$  day interaction [ $F_{\text{interaction}(12,90)} = 3.335, p < 0.0005$ ] compared to the vehicle group. The administration of SCFAs induced a significant reduction of ethanol intake compared to both the NaCl and the vehicle groups. (B) Ethanol preference was expressed as a percentage of total fluid intake, calculated as the sum of daily alcohol and water consumption. Two-way ANOVA (treatment  $\times$  day) revealed significant effect of treatment [ $F_{\text{treatment}(2,15)} = 3008, p < 0.0001$ ], day [ $F_{\text{day}(3927, 58.91)} = 3.382, p < 0.01$ ], but not significant interaction compared to the vehicle group. Tukey post hoc indicate that the administration of SCFAs induced a significant reduction of ethanol preference. (C) Water intake is expressed in mL/kg body weight/day. We observed a significant effect of treatment [ $F_{\text{treatment}(2,15)} = 401.0, p < 0.0001$ ] compared to the vehicle group. The administration of SCFAs induced a significant increase in water intake compared to the vehicle group. (D) Total fluid intake is expressed in mL/kg body weight/day, and weight is expressed in grams. The administration of SCFAs did not induce a significant change in total fluid intake [ $F_{\text{treatment}(2,15)} = 0.2688, p:0.76$ ] or in body weight [ $F_{\text{treatment}(2,15)} = 0.3229, p:0.72$ ] compared to the vehicle group. Note that body weight did not differ among the three groups of rats before alcohol access (Mean  $\pm$  SEM: SCFA group  $299 \pm 9.34$  g, NaCl group  $291 \pm 3.4$  g, and vehicle group  $285 \pm 1.85$  g; one-way ANOVA  $F_{\text{treatment}(2,45)} = 1.448, p:0.2458$ , N.S.). Male UChB rats voluntarily consuming a 10% ethanol solution for 58 days were treated with the same combination of SCFAs, 554 mg/kg NaCl solution, or vehicle, by oral gavage twice-daily for five days. (E) Ethanol intake is expressed in g/kg body weight/day. We observed a significant effect of treatment [ $F_{\text{treatment}(2,15)} = 8.811, p < 0.01$ ], day [ $F_{\text{day}(5202, 78.02)} = 81.86, p < 0.0001$ ] and a significant treatment  $\times$  day interaction [ $F_{\text{interaction}(28,210)} = 94.80, p < 0.0001$ ] compared to the vehicle group. The administration of SCFAs induced a significant reduction in ethanol intake compared to both the NaCl and the vehicle groups. (F) Ethanol preference was expressed as a percentage of total fluid intake, calculated by adding alcohol and water consumption. Two-way ANOVA (treatment  $\times$  day) revealed significant effect of treatment [ $F_{\text{treatment}(2,15)} = 67.17, p < 0.0001$ ], day [ $F_{\text{day}(5625, 39.37)} = 115.7, p < 0.0001$ ] and significant interaction [ $F_{\text{interaction}(8,60)} = 146.8, p < 0.0001$ ], compared to the vehicle group. Tukey post hoc indicate that the administration of SCFAs induced a significant reduction of ethanol preference compared to the vehicle and NaCl groups. (G) Water intake is expressed in mL/kg body weight/day. We observed a significant effect of treatment [ $F_{\text{treatment}(2,15)} = 61.50, p < 0.0001$ ], day [ $F_{\text{day}(2757, 41.36)} = 103.9, p < 0.0001$ ] and a significant treatment  $\times$  day interaction [ $F_{\text{interaction}(8,60)} = 128.1, p < 0.0001$ ] compared to the vehicle group. The administration of SCFAs induced a significant increase in water intake compared to the vehicle group. (H) Total fluid intake is expressed in mL/kg body weight/day, and weight is expressed in grams. The administration of SCFAs did not induce a significant change in total fluid intake [ $F_{\text{treatment}(2,15)} = 0.8664, p:0.44$ ] or in body weight [ $F_{\text{treatment}(2,15)} = 0.06547, p:0.93$ ] compared to the vehicle group. Arrows indicate intragastric administration of SCFAs, NaCl, or vehicle. Data are presented as mean  $\pm$  SEM. N = 6 animals per group. Two-way ANOVA followed by Tukey *post-hoc* tests, \*\*\* $p < 0.0001$ .

suggests that the observed behavioral effect on ethanol intake is attributable to SCFAs administration rather than to any nonspecific discomfort. Note that no significant differences were found in body weight among the three groups of rats before ethanol access (Fig. 1D).

### **Chronic voluntary alcohol intake is markedly inhibited by intragastric co-administration of three SCFAs**

Subsequently, we evaluated whether intragastric co-administration of SCFAs would also reduce voluntary ethanol intake, but now in animals that had been drinking alcohol chronically. In these studies, male UChB rats were maintained with free access to 10% ethanol solution and water for 58 days to induce chronic ethanol dependence, leading to a voluntary ethanol intake of 9 g/kg/day (Fig. 1E). At that time, animals were divided into three experimental groups and treated with (1) a combination of SCFAs containing 300 mg/kg sodium acetate, 300 mg/kg sodium propionate and 300 mg/kg sodium butyrate; (2) NaCl at a dose of 554 mg/kg containing the same molar concentration of sodium as that received by the animals treated with SCFAs; or (3) distilled water. All treatments were administered by oral gavage twice-daily for five days. The administration of SCFAs led to a very strong reduction in chronic ethanol intake ( $\sim 93\%$ ,  $p < 0.0001$ ) (Fig. 1E) and ethanol preference ( $p < 0.0001$ ) (Fig. 1F) compared to the control groups. This effect did not appear immediately after SCFAs treatment but occurred with a lag time of about three days following the first SCFAs dose administration. Once again, SCFAs administration induced a significant increase in water intake ( $p < 0.0001$ ) (Fig. 1G), normalizing animal's hydric homeostasis without affecting animal body weight (Fig. 1H).

### **Intragastric co-administration of three SCFAs reduces ethanol-induced intestinal and hepatic inflammation and restores normal intestinal architecture**

Then, we evaluate whether SCFAs administration could reduce ethanol-induced intestinal alterations. For this, samples of proximal colon were obtained 24 h after the last SCFAs or vehicle administration. At histological level, we observed that chronic alcohol intake induced a significant increase ( $p < 0.0001$ ) in the length of the intestinal crypts (Fig. 2A and B), one of the common markers of intestinal damage<sup>33</sup>, and a significant increase ( $p < 0.01$ ) in lamina propria cell infiltration in the colonic mucosa (Fig. 2C and D) compared to ethanol-naïve animals. However, SCFAs administration completely normalized the length of the intestinal crypts ( $p < 0.0001$ ) (Fig. 2A and B), and lamina propria cell infiltration ( $p < 0.0001$ ) (Fig. 2C and D) compared to vehicle-treated animals.

Additionally, we evaluated the ratio of proliferating cells in the lamina propria of the proximal colon samples. Proliferating cell nuclear antigen (PCNA) positivity was significantly reduced ( $p < 0.01$ ) in animals chronically drinking ethanol and treated with SCFAs compared to animals chronically drinking ethanol and treated with the vehicle (Supplementary Fig. 1A and B). Then, we evaluated if PCNA-positive areas in the lamina propria correlated with cell infiltrate density, as a surrogate for proliferation rate. We observed a direct association between cell infiltrate density and PCNA-positive areas (Supplementary Fig. 1C), suggesting that infiltrating cells are actively proliferating and potentially contributing to epithelial barrier disruption, as previously reported<sup>34</sup>.

Ethanol-induced intestinal inflammation was further corroborated measuring the mRNA levels of pro-inflammatory cytokines by RT-qPCR in samples of proximal colon. Chronic ethanol intake induced a significant increase in the expression levels of IL1 $\beta$ , IL8 and TNF- $\alpha$  ( $p < 0.01$ ) compared to ethanol-naïve animals, while SCFAs administration restored these levels to normal levels ( $p < 0.05$ ) (Fig. 2E).

We further evaluated whether ethanol-induced intestinal alterations could lead to an increased intestinal LPS permeability and the concomitant increase in liver inflammation. For this, plasma LPS levels were measured by ELISA, while hepatic inflammation was evaluated by RT-qPCR. We observed that chronic ethanol intake induced a significant increase ( $p < 0.01$ ) in plasma LPS levels (Fig. 3A), which was associated with a significant increase in the hepatic expression levels of the LPS-binding protein (LBP) ( $p < 0.001$ ) and the pro-inflammatory cytokines IL1 $\beta$  ( $p < 0.0001$ ), and TNF- $\alpha$  ( $p < 0.001$ ) (Fig. 3B) compared to ethanol-naïve animals. However, SCFAs administration completely abolished the ethanol-induced increase in plasma LPS levels ( $p < 0.01$ ) (Fig. 3A) and reduced the ethanol-induced increase in hepatic LBP ( $p < 0.01$ ), IL1 $\beta$  ( $p < 0.05$ ) and TNF- $\alpha$  ( $p < 0.05$ ) expression levels (Fig. 3B).

### **Intragastric co-administration of three SCFAs reduces ethanol-induced neuroinflammation**

To assess ethanol-induced neuroinflammation, astrocyte and microglia morphology was evaluated by immunofluorescence in the hippocampus. As previously reported<sup>35</sup>, chronic alcohol intake induced a significant increase in astrocyte and microglial activation, evidenced by a significant increase in astrocyte surface area ( $p < 0.05$ ) (Fig. 4A, B and E), total length of astrocytic processes ( $p < 0.05$ ) (Fig. 4A, B and F), the astrocytic ramification index ( $p < 0.01$ ) (Fig. 4A, B and G), and the microglial solidity ( $p < 0.05$ ) (Fig. 4C, D and H) compared to ethanol-naïve animals. In contrast, SCFA administration significantly reduced ethanol-induced increase in astrocyte surface area ( $p < 0.01$ ) (Fig. 4A, B and E), total length of astrocytic processes ( $p < 0.01$ ) (Fig. 4A, B and F), and the microglial solidity ( $p < 0.0001$ ) (Fig. 4C, D and H), while no effects were observed at the level of astrocytic ramification index (Fig. 4A, B and G).

### **Intragastric co-administration of three SCFAs reduces alterations in the transcriptional dynamics of the nucleus accumbens induced by chronic ethanol intake**

The nucleus accumbens has repeatedly been demonstrated to be a key component of the circuitry associated with excessive alcohol consumption<sup>36</sup>. To explore the gene regulatory mechanisms in UChB animals chronically drinking ethanol, and how this pattern changes upon SCFAs administration, we performed an RNA-Seq analysis. In the comparison of ethanol-naïve vs chronic ethanol intake, we found 367 differentially expressed genes (DEGs) at the adjusted  $p < 0.05$ , with 206 up-regulated and 161 down-regulated (Fig. 5A). For chronic ethanol intake vs SCFAs condition, 63 DEGs were found, with 5 up-regulated and 58 down-regulated ( $p < 0.05$ ; Fig. 5B), while

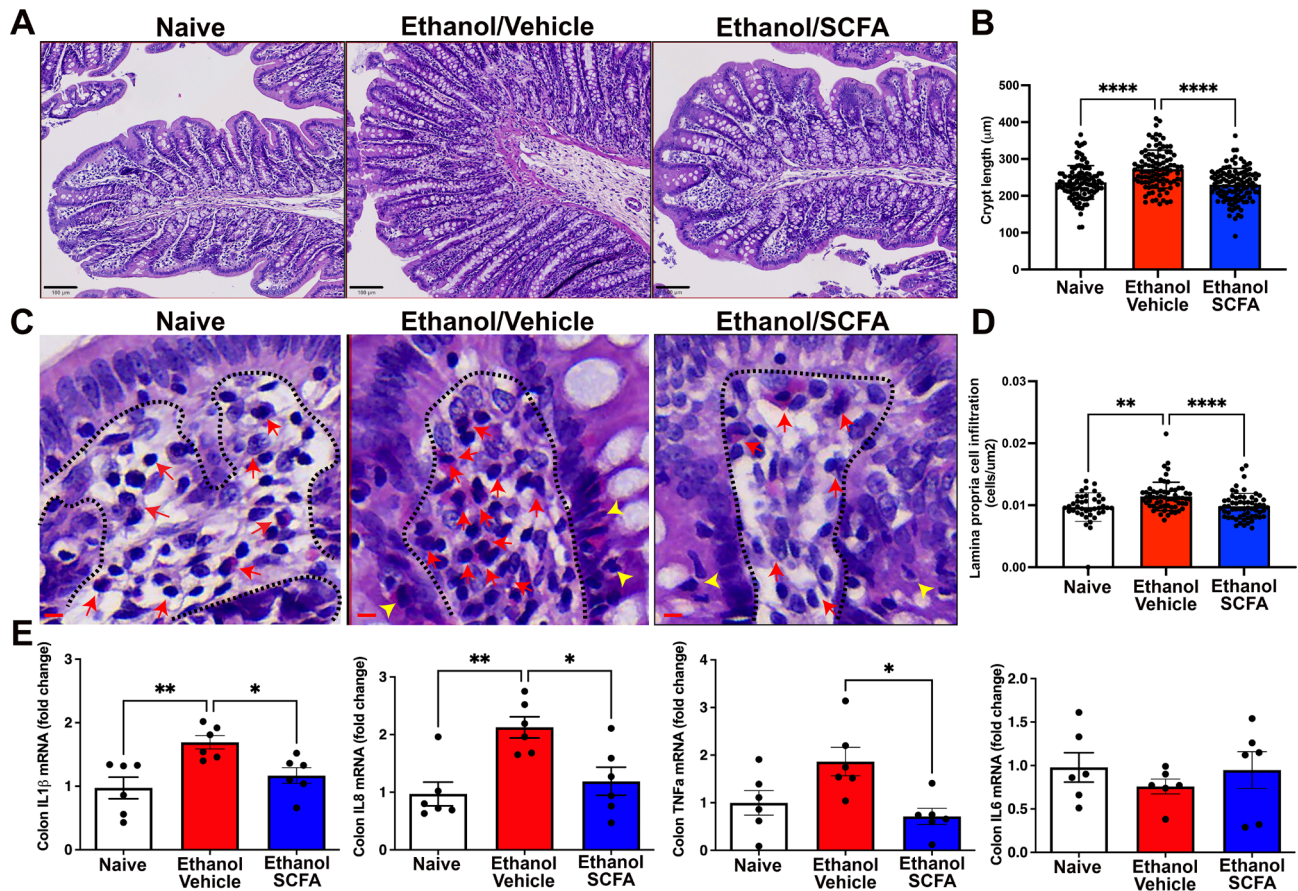


**Fig. 2.** Intragastric administration of SCFAs to animals chronically consuming ethanol restores normal intestinal architecture and reduces ethanol-induced inflammation in the proximal colon. Male UChB rats, voluntarily consuming a 10% ethanol solution for 58 days, were treated with either a combination of SCFAs (300 mg/kg each sodium acetate, sodium propionate and sodium butyrate), or 554 mg/kg NaCl solution (vehicle), by oral gavage twice-daily for five days. An additional group of untreated animals drinking only water (naïve) was used as a control. (A) Representative haematoxylin & eosin staining of proximal colon tissue showing crypts length. (B) Quantification of crypt length. (C) Representative hematoxylin & eosin staining of proximal colon tissue showing lamina propria cell infiltration, with dashed black line separating epithelial lining from lamina propria compartments. Red arrows point to polymorphonuclear and eosinophil leukocytes, plasma cells and macrophages, based on morphological identification. Yellow arrows point to intraepithelial polymorphonuclear cell infiltration. Scale bar 10 μm. (D) Quantification of lamina propria cell infiltration in the colonic mucosa. (E) Quantification of mRNA levels of the pro-inflammatory cytokines IL-1β, IL-8, TNF-α and IL-6 determined by RT-qPCR in samples of proximal colon. Data are presented as mean ± SEM. N=6 animals per group. \*p < 0.05; \*\*p < 0.01; \*\*\*p < 0.0001, One-way ANOVA followed by Bonferroni post-hoc test.

for the ethanol-naïve vs SCFAs conditions, 105 DEGs were found, with 59 up-regulated and 46 down-regulated ( $p < 0.05$ ; Fig. 5C). The clustering heatmap of DEGs presented the differences in the transcriptomic profiles between the different experimental conditions (Supplementary Fig. 2A, B, and C). In the two most important comparisons (Ethanol-Naïve vs. Chronic Ethanol and Chronic Ethanol vs. SCFAs), we identified a total of 35 common differentially expressed genes. The expression of these genes was altered in the ethanol condition, but their expression levels were restored when chronic ethanol drinking animals were treated with SCFAs (Fig. 5D). The full list of all significantly regulated genes in all comparison is presented in Supplementary Table 2.

The differentially expressed genes underwent Gene-Ontology (GO) pathway enrichment analysis, classifying the up- and down-regulated genes. In the GO terms analysis for the Ethanol-Naïve vs chronic ethanol samples, we found up-regulated genes involved in biological processes such as “Response to endoplasmic reticulum stress” and “Regulation of cytosolic calcium ion concentration”. Importantly, genes involved in “Synapse organization”; “Response to toxic substances” and “Negative regulation of neuron apoptotic process”, were found to be down-regulated (Fig. 5E). Conversely, for the chronic ethanol vs SCFAs conditions, down-regulated genes were associated with “Regulation of behavior” and “Central nervous system development” (Fig. 5F). For the ethanol-Naïve vs SCFAs conditions, we found up-regulated genes involved in processes such as “Positive regulation of protein kinase B signaling” and “Response to glucocorticoid” (Fig. 5G). Altogether, these data demonstrated that chronic ethanol intake leads to marked transcriptional changes, and that SCFAs treatment attenuates some of the molecular phenotypes.

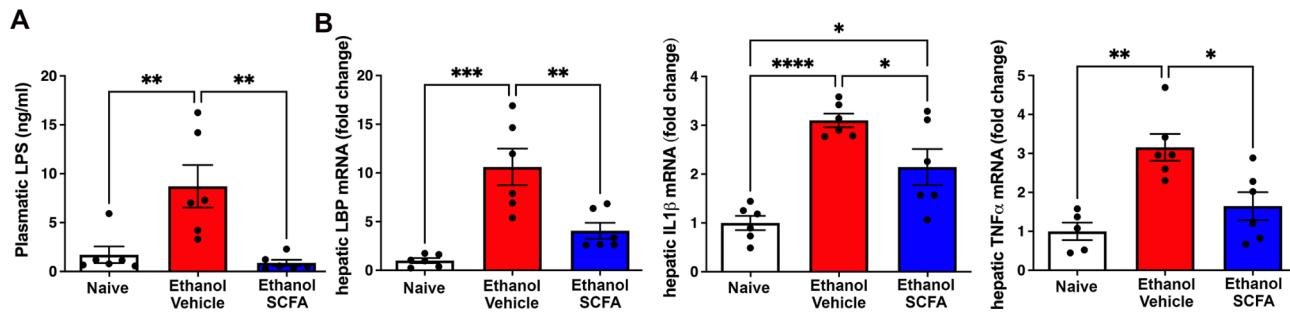


**Fig. 3.** Intragastric administration of SCFAs reduces both plasma LPS levels and liver inflammation induced by chronic ethanol consumption. Male UChB rats, voluntarily drinking a 10% ethanol solution for 58 days were treated with either a combination of SCFAs (300 mg/kg each sodium acetate, sodium propionate and sodium butyrate), or ii) 554 mg/kg NaCl solution (vehicle), by oral gavage twice-daily for five days. An additional group of untreated animals drinking only water (naïve) was used as a control. (A) Plasmatic levels of LPS were determined by ELISA. (B) mRNA levels of the LPS binding protein (LBP) and the pro-inflammatory cytokines IL-1 $\beta$  and TNF- $\alpha$  were determined by RT-qPCR in hepatic samples. Data are presented as mean  $\pm$  SEM. N = 6 animals per group. \* $p$  < 0.05; \*\* $p$  < 0.01; \*\*\* $p$  < 0.001; \*\*\*\* $p$  < 0.0001, One-way ANOVA followed by Bonferroni post-hoc test.

### Sodium butyrate is the most potent SCFA in reducing chronic voluntary ethanol intake

Then, we wanted to know which of the SCFAs is the most potent in reducing chronic voluntary ethanol intake. For this, a new group of male UChB rats was maintained with free access to 10% (v/v) ethanol solution and water for 45 days, and at that time, animals were divided into five groups and treated with either (1) a combination of SCFAs containing 300 mg/kg sodium acetate, 300 mg/kg sodium propionate and 300 mg/kg sodium butyrate; (2) 300 mg/kg sodium butyrate; (3) 300 mg/kg sodium propionate; (4) 300 mg/kg sodium acetate or (5) distilled water. All treatments were administered by oral gavage twice-daily for five days. When administered alone, all SCFAs were able to significantly reduce chronic voluntary ethanol intake compared to the vehicle-treated animals (Fig. 6A). However, the most potent therapeutic effect was achieved by sodium butyrate, which induced a ~ 72% reduction in ethanol intake compared to the vehicle-treated rats ( $p$  < 0.0001), an effect that was significantly more potent than the ~ 48% reduction induced by sodium propionate and sodium acetate ( $p$  < 0.001) (Fig. 6A). Once butyrate was identified as the most potent SCFA, we performed a dose-response curve to determine which is the optimal butyrate dose to reduce voluntary alcohol intake. For this, a new group of male UChB rats was given free access to 10% ethanol solution and water for 64 days, and at that time, animals were divided into four groups and treated either with (1) 300 mg/kg sodium butyrate; (2) 30 mg/kg sodium butyrate; (3) 3 mg/kg sodium butyrate or (4) distilled water. All treatments were administered by oral gavage twice-daily for five days. We observed that intragastric administration of 300 mg/kg sodium butyrate induced the strongest therapeutic effect, leading to an ~ 89% reduction in voluntary ethanol intake ( $p$  < 0.0001) compared to vehicle-treated animals, while intragastric administration of 30 mg/kg sodium butyrate induced a ~ 51% reduction in voluntary ethanol intake ( $p$  < 0.0001), and the administration of 3 mg/kg sodium butyrate had no therapeutic effect (Fig. 6B). For both the 300 mg/kg and 30 mg/kg sodium butyrate doses, the therapeutic effect was completely lost three days after treatment discontinuation (Fig. 6B).

### Sodium butyrate increases histone acetylation

It has been reported that sodium butyrate can act as a potent inhibitor of the histone deacetylase activity, leading to histone hyperacetylation and changes in gene expression<sup>37</sup>. Thus, we measured histone acetylation level by Western blot both in the striatum and the prefrontal cortex, since these brain areas play a key roles in mediating the acute and chronic effects of drugs of abuse<sup>38</sup>. As expected, two daily doses of 300 mg/kg sodium butyrate for five days to animals that have been drinking ethanol chronically induced a significant increase in the levels of H3 histone acetylation in the striatum ( $p$  < 0.05) (Fig. 7A–C and Supplementary Fig. 3A) and in the prefrontal cortex ( $p$  < 0.05) (Fig. 7D–F and Supplementary Fig. 3B) compared to ethanol-drinking animals treated with the vehicle and ethanol-naïve animals, indicating that intragastrically administered sodium butyrate is able to reach the brain and induce an increase in histone acetylation.

### Discussion

Increasing evidence suggests a role of altered gut microbiota as contributor to the development of gut, liver, and brain inflammation in the context of alcohol dependence<sup>39</sup>. Thus, a healthy microbiota community is essential for the normal regulation of the microbiota-gut-brain axis. Amongst the most important and pleiotropic components of microbe-to-host signaling highlights SCFAs (acetate, propionate and butyrate)<sup>40</sup>, and a reduction of SCFAs-producing bacteria associates with increased alcohol intake<sup>41</sup>. However, the underlying mechanisms through which SCFAs might influence brain physiology and behavior have not been fully elucidated.

Here we show that twice-daily intragastric administration of SCFAs for six days to male ethanol-naïve UChB rats (bred for generations for high ethanol intake), completely prevented the initiation phase of alcohol intake, evidenced by a ~ 85% reduction in voluntary ethanol intake compared with animals treated with NaCl or vehicle.

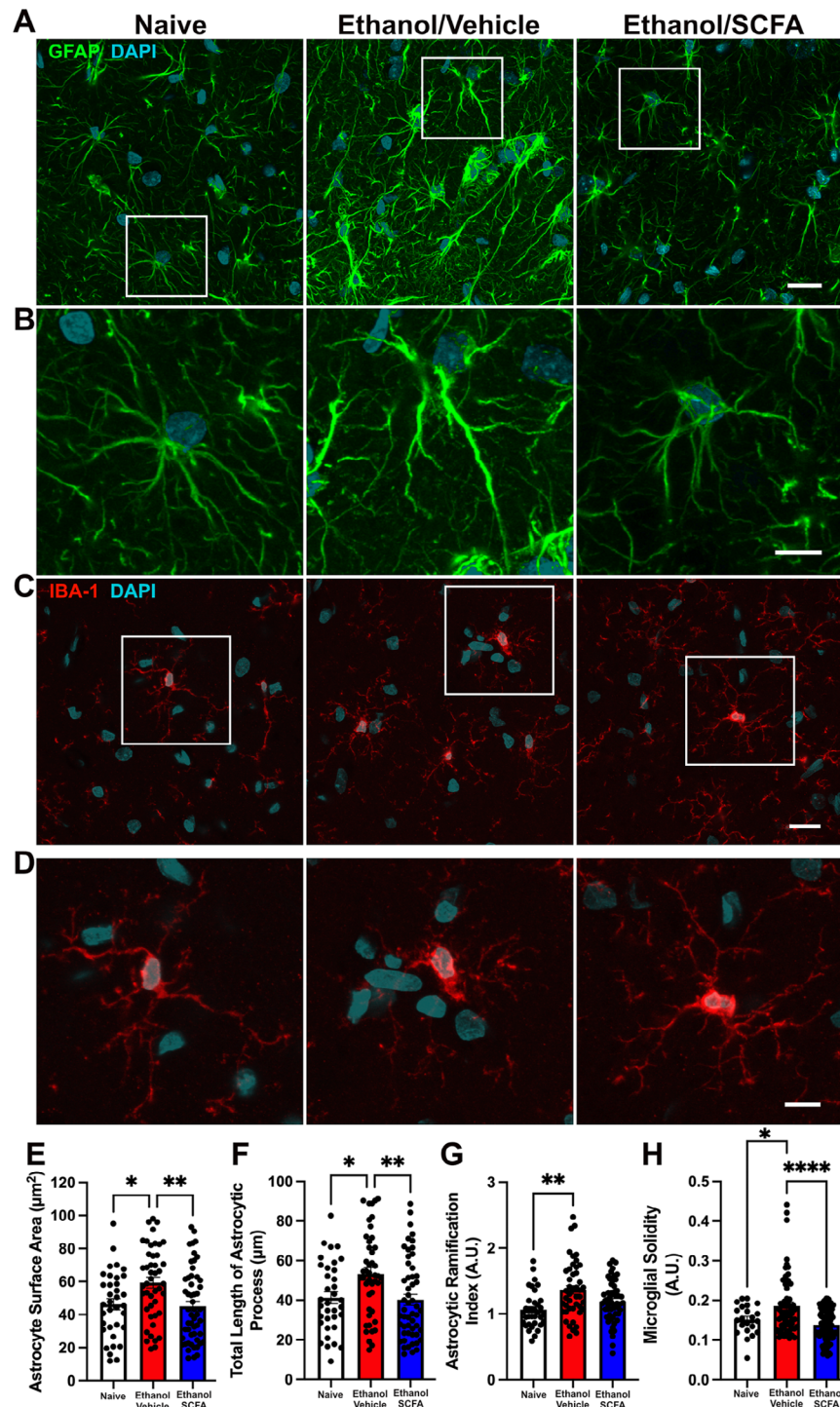


**Fig. 4.** Intragastric Administration of SCFAs Reduces Ethanol-Induced Neuroinflammation. Male UChB rats, voluntarily consuming 10% ethanol for 58 days, were treated with either: (1) a combination of SCFAs (300 mg/kg each of sodium acetate, sodium propionate, and sodium butyrate) or (2) a sodium chloride (NaCl) solution (554 mg/kg, vehicle) by oral gavage twice daily for five days. A third group of untreated animals drinking only water (naïve) was used as a control. (A) Representative confocal micrographs showing GFAP immunoreactivity (green) in the CA1 *stratum radiatum* of the hippocampus under the three experimental conditions. Nuclei are counterstained with DAPI (cyan). Scale bar: 25  $\mu\text{m}$ . (B) Magnified view of the region highlighted by the rectangle in (A). Scale bar: 10  $\mu\text{m}$ . (C) Microglial Iba-1 immunoreactivity (red) and DAPI (cyan). Scale bar: 25  $\mu\text{m}$ . (D) Magnified view of the region highlighted by the rectangle in (C). (E) Quantification of astrocyte surface area. (F) Quantification of the total length of astrocytic processes. (G) Quantification of the astrocytic ramification index. (H) Quantification of microglial solidity. Data are presented as mean  $\pm$  SEM based on six microphotographs/hemisphere (N = 6 animals per group). Statistical significance was determined using one-way ANOVA followed by Bonferroni post-hoc test. \* $p < 0.05$ , \*\* $p < 0.01$ , \*\*\* $p < 0.0001$ .

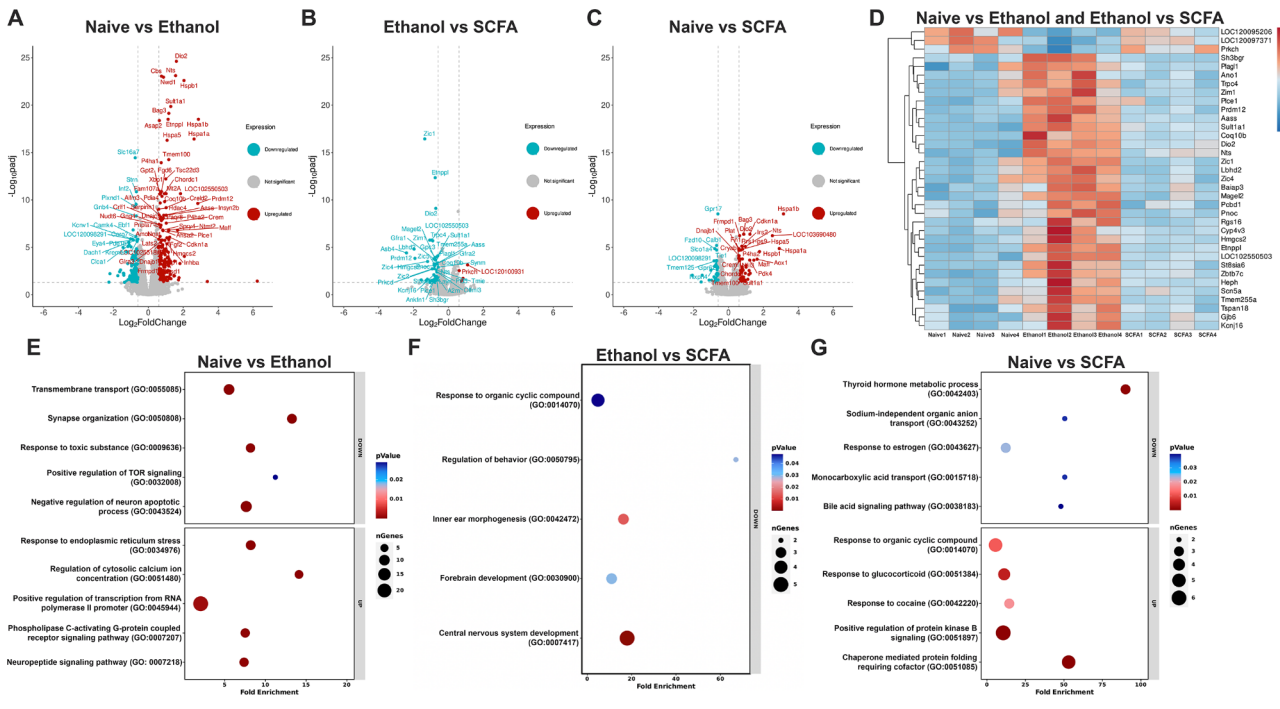


**Fig. 5.** Transcriptional dynamics in the nucleus accumbens of animals chronically drinking ethanol treated with the SCFAs combination or the vehicle. Male UChB rats, voluntarily consuming a 10% ethanol solution for 58 days, were treated with either a combination of SCFAs (300 mg/kg each sodium acetate, sodium propionate and sodium butyrate) or 554 mg/kg NaCl solution (vehicle), by oral gavage twice-daily for five days. An additional group of untreated animals drinking only water (naïve) was used as a control. After the last administration animals were euthanized and the nucleus accumbens was dissected for RNA-seq determinations. (A–C) Volcano plots of differentially expressed genes display the up-regulated (red dots) and down-regulated (light blue dots) genes. Gray dots indicate no significant changes among the different conditions for (A) Ethanol-Naïve vs. Chronic Ethanol conditions, (B) Chronic Ethanol vs. SCFAs conditions and (C) Ethanol-Naïve vs. SCFAs conditions. (D) Heatmap of the differentially expressed genes that were found common among Ethanol-Naïve vs. Chronic Ethanol and Chronic Ethanol vs. SCFAs conditions. (E–G) Bubble plots representing the functional enrichment analysis of differentially expressed genes. GO biological processes terms were classified based on up- and down-regulated expression changes. Only GO terms with a p-value < 0.05 were included in the analysis for (E) Ethanol-Naïve vs Chronic Ethanol conditions, (F) Chronic Ethanol vs SCFA conditions and (G) Ethanol-Naïve vs SCFAs conditions. Data were obtained from four animals per experimental condition.

Similarly, twice-daily intragastric administration of SCFAs to UChB animals that had been voluntarily drinking ethanol for 58 days leads to a marked reduction in voluntary ethanol intake (~ 93%) compared to vehicle-treated animals. This indicates that SCFAs administration can prevent the initiation of alcohol intake and strongly reduce chronic alcohol intake once the addictive behavior is already established. These results agree with reports showing that ad libitum sodium butyrate supplementation in drinking water reduced ethanol preference in C57BL/6 J mice<sup>42</sup>, while intraperitoneal administration of sodium butyrate to alcohol-dependent rats decreased ethanol consumption in the operant ethanol self-administration paradigm<sup>43</sup>. These therapeutic effects of SCFA administration have also been reported for animal models of morphine<sup>44</sup> and cocaine<sup>45</sup> dependence. Thus, highlighting the therapeutic potential of SCFAs administration to reduce the seeking behavior induced by the chronic use of several drugs of abuse.

The molecular mechanisms underlying alcohol-drinking behavior are multifaceted and shared between males and females<sup>46</sup>. In our animal model, chronic alcohol intake alters the intestinal architecture, as evidenced by increased intestinal crypt length, and induces intestinal inflammation, as evidenced by an increase in colonic leukocyte infiltration and pro-inflammatory cytokines transcript levels. Indeed, increased intestinal levels of pro-inflammatory cytokines, including TNF- $\alpha$ , downregulate tight junction protein expression and cause disruption of the gut barrier<sup>47</sup>. Furthermore, TNF- $\alpha$  is highly expressed in lamina propria macrophages from duodenal biopsies of alcoholics patients<sup>48</sup>, possibly contributing to gut barrier alterations. Accordingly, in our animal model SCFAs administration completely restored normal intestinal structure and strongly reduced colonic inflammation. Many studies have shown that SCFAs, especially butyrate, can act as anti-inflammatory agents at the intestinal level<sup>26,39,49</sup>. These studies, both in human and in animal models, have shown that the pro-inflammatory cytokines TNF- $\alpha$ , IL-1 $\beta$ , IL-6, and IL-8 are inhibited in response to SCFAs administration<sup>26,39,49</sup>. The mechanism underlying the anti-inflammatory effects of SCFAs involves, at least in part, NF- $\kappa$ B inhibition<sup>39,50</sup>, by rescuing the redox machinery that controls reactive oxygen species mediating NF- $\kappa$ B activation<sup>25</sup>.

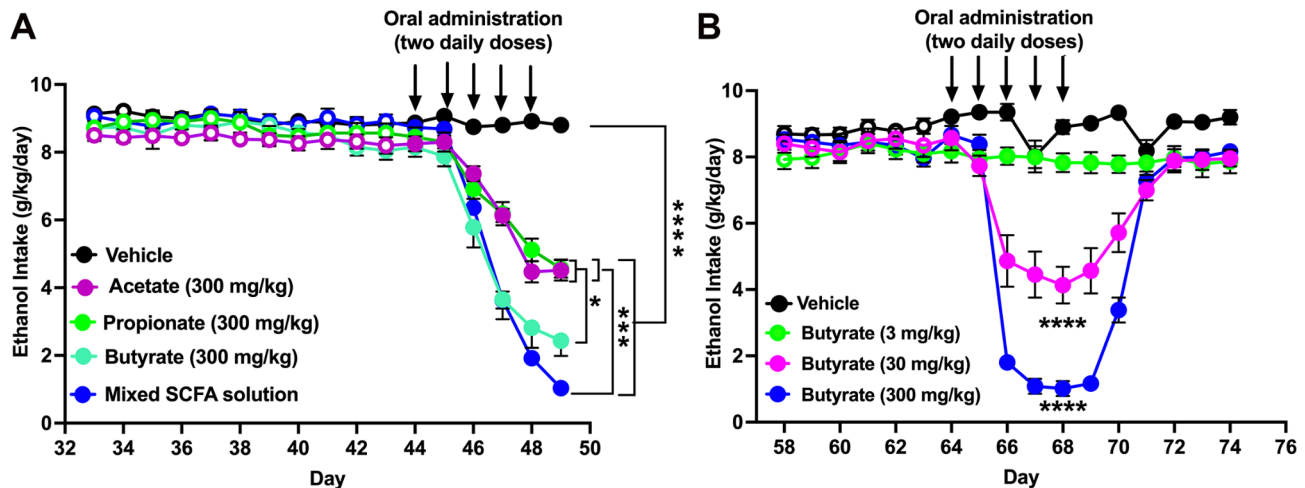


**Fig. 6.** Sodium butyrate is the most potent SCFA in reducing chronic voluntary ethanol intake, produced in a dose-dependent manner. (A) Male UChB rats, voluntarily consuming a 10% ethanol solution for 44 days, were treated with either (1) a combination of SCFAs (300 mg/kg each sodium acetate, sodium propionate and sodium butyrate), (2) 300 mg/kg sodium acetate; (3) 300 mg/kg sodium propionate; (4) 300 mg/kg sodium butyrate, or (5) vehicle by oral gavage twice-daily for five days. Ethanol intake was expressed as g/kg body weight/day. Arrows indicate intragastric administrations. We observed a significant effect of treatment [ $F_{\text{treatment}(4,25)} = 8.216, p < 0.001$ ], day [ $F_{\text{day}(3418, 85,46)} = 452.9, p < 0.0001$ ] and a significant treatment  $\times$  day interaction [ $F_{\text{interaction}(64,400)} = 39.65, p < 0.0001$ ] compared to the vehicle group. Sodium butyrate administration produces a significantly greater reduction in ethanol consumption than sodium acetate ( $*p < 0.05$ ), sodium propionate ( $*p < 0.05$ ), and the vehicle ( $****p < 0.0001$ ). (B) Male UChB rats voluntarily consuming a 10% ethanol solution for 63 days were treated with either (1) 300 mg/kg sodium butyrate; (2) 30 mg/kg sodium butyrate; (3) 3 mg/kg sodium butyrate; or (4) vehicle by oral gavage twice-daily for five days. Ethanol intake was expressed as gr/kg body weight/day. We observed a significant effect of treatment [ $F_{\text{treatment}(3,20)} = 46.42, p < 0.0001$ ], day [ $F_{\text{day}(2339, 46,78)} = 128.8, p < 0.0001$ ] and a significant treatment  $\times$  day interaction [ $F_{\text{interaction}(24,160)} = 48.54, p < 0.0001$ ] compared to the vehicle group. The reduction of ethanol intake induced by a dose of 300 mg/kg of sodium butyrate, compared to that of the vehicle group, is significantly greater than that induced by 30 mg/kg and by that 3 mg/kg sodium butyrate. Arrows indicate intragastric administrations. Data are presented as mean  $\pm$  SEM. N = 6 animals per group. Two-way ANOVA followed by Tukey post-hoc tests,  $*p < 0.05$ ,  $****p < 0.0001$ .

Ethanol-induced intestinal inflammation and the concomitant alteration of intestinal structure results in increased gut permeability, facilitating the translocation of intestinal microbiota components, in particular LPS, to the portal circulation, inducing systemic and liver inflammation<sup>51</sup>. In the present study, chronic ethanol intake increased plasma LPS levels and the expression of pro-inflammatory molecules in the liver, which were restored to normal levels by SCFAs administration. It has been previously reported that in rats, the administration of SCFAs decreased ethanol-induced liver damage and hepatic inflammation<sup>52</sup>. Moreover, SCFAs play an important role in gut barrier integrity maintenance, blocking LPS translocation by increased mucin 2 expression, enhancing the protection of the mucosal layer<sup>53</sup>. Furthermore, butyrate increases the expression of tight junction proteins to minimize paracellular permeability<sup>54</sup>. Therefore, these effects could be responsible for the reduction of plasmatic LPS levels observed in SCFAs-treated animals, and the concomitant reduction in the expression level of pro-inflammatory molecules in the liver.

A limitation of our study is that we were unable to measure fecal SCFAs content, which would confirm SCFA delivery to the colon. However, a prior study by Xia et al.<sup>55</sup>, using gas chromatographic analysis, demonstrated that rats treated with propionic acid by oral gavage—at a dose similar to that used in our study (300 mg/kg, twice daily)—had significantly higher levels of propionic acid in the proximal colon compared to the control group. Given that propionate, acetate, and butyrate were administered at the same dose and frequency in the present study as propionate in Xia et al., it is highly likely that all SCFAs reached the proximal colon in this study as well.

Since the small intestine expresses moderate levels of SCFA transporters compared to the colon<sup>56</sup> and based on the histological and molecular improvements observed in our model, we suggest that colonic SCFA levels were sufficient to exert protective effects against ethanol-induced colonic damage.

Microglia and astrocytes are the primary immune surveillance cells in the brain, and their activation, which can be evaluated by changes in their morphological shapes, is considered a hallmark of neuroinflammation<sup>57,58</sup>. Several studies suggest that microglia and astrocytes play important roles in chronic ethanol intake, particularly in the hippocampus, as this brain area is the most pathologically affected by chronic ethanol consumption, both in humans<sup>59,60</sup> and in animal models<sup>39,61–63</sup>. Furthermore, increased levels of glial activation and inflammatory cytokines have been observed in the post-mortem human hippocampus of long-term alcohol users. This neuroinflammation, along with concomitant neuronal damage, has been proposed to be responsible for the loss of control over drinking and severe intoxication<sup>64,65</sup>. Accumulating evidence suggests that SCFAs

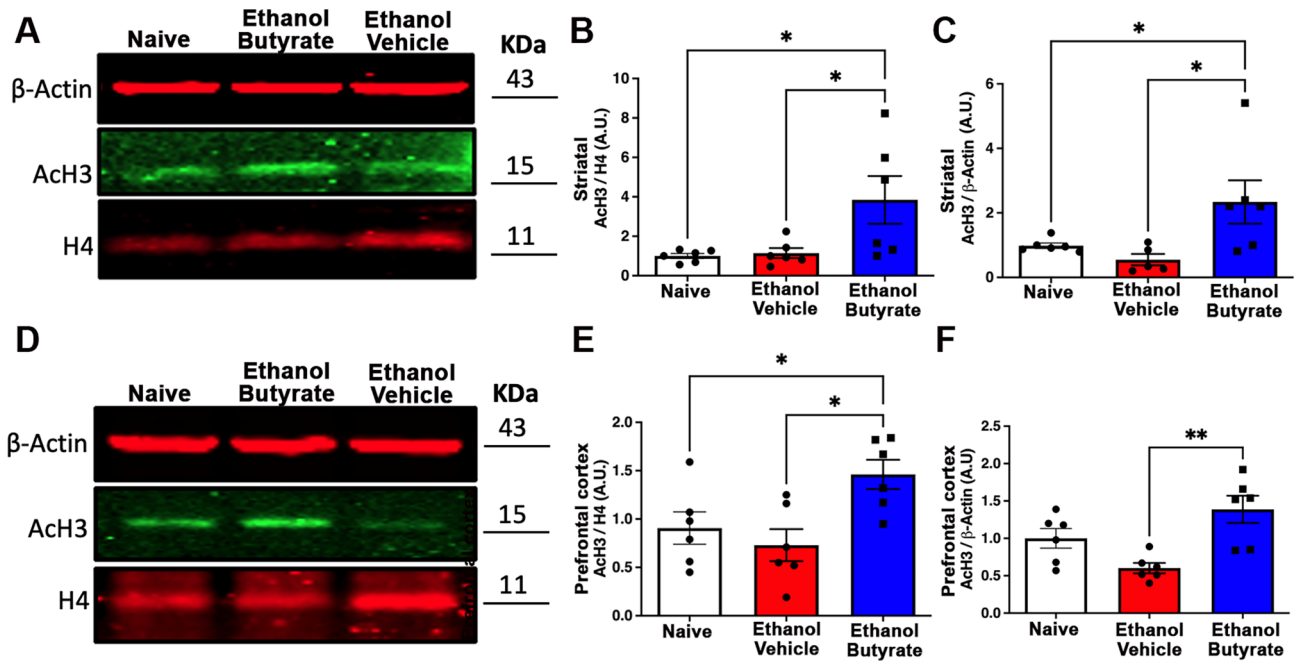


**Fig. 7.** Sodium butyrate increases H3 histone acetylation levels in the striatum and prefrontal cortex. Male UChB rats, voluntarily consuming a 10% ethanol solution for 44 days, were treated with either 300 mg/kg sodium butyrate or vehicle by oral gavage twice-daily for five days. An additional group of untreated animals drinking only water (naïve) was used as a control. (A) Representative Western Blot showing striatal levels of H3 histone acetylation (AcH3). Histone H4 and β-actin were used as housekeeping genes. (B) Quantification of striatal AcH3 levels normalized to the nuclear marker histone H4. (C) Quantification of striatal AcH3 levels normalized to the housekeeping gene β-actin. (D) Representative Western Blot showing prefrontal cortex levels of H3 histone acetylation (AcH3). (E) Quantification of prefrontal cortex AcH3 levels normalized to the nuclear marker histone H4. (F) Quantification of prefrontal cortex AcH3 levels normalized to β-actin. Data are presented as mean  $\pm$  SEM. N = 6 animals per group. \* $p$  < 0.05, \*\* $p$  < 0.01. One-way ANOVA followed by Bonferroni post-hoc test.

can cross the blood–brain-barrier, reaching the CNS<sup>66</sup>, having neuroactive properties<sup>67</sup> not only in neurons but also in astrocytes and microglia. Here we showed that, as previously reported<sup>35</sup>, chronic alcohol intake induced a significant increase in hippocampal astrocyte and microglial activation. However, these alterations were completely reversed in SCFAs-treated animals. Several studies have reported that SCFAs are able to decrease microglial and astrocyte activation and pro-inflammatory cytokine secretion<sup>39,68</sup>. Additionally, butyrate treatment induces morphological and functional changes in microglia towards a homeostatic profile<sup>69</sup>. Although the precise mechanism involved in SCFA effects on microglial and astrocytes remains unclear, it has been reported that these cells express the SCFA receptor GPR109a, which upon activation, can induce anti-inflammatory effects by downregulating NF-κB activation<sup>70</sup>.

While many brain areas contribute to drug reward and to the development of addiction, the nucleus accumbens is a key component of the circuitry associated with excessive alcohol consumption<sup>71</sup>, making it an attractive neurobiological area to evaluate the molecular effects associated to chronic alcohol intake. In agreement, we observed that chronic alcohol-drinking animals treated with the vehicle had the highest number of differentially expressed genes in this brain area, with 206 up-regulated and 161 down-regulated genes compared to ethanol-naïve animals. Among down-regulated genes it could be observed genes associated to synapse organization, response to toxic substances, and negative regulation of neuron apoptotic process, among others. Alteration in the expression levels of some of these genes, including genes associated to synaptic function, have also been reported in RNA-Seq data obtained from postmortem brains of alcoholic patients<sup>72</sup> and from the nucleus accumbens of rhesus macaques drinking alcohol chronically<sup>36</sup>. Interestingly, SCFAs administration reversed most of the transcriptional effects induced by alcohol intake, suggesting that SCFAs treatment leads to normalization of transcriptional regulation, counteracting specific neuro-adaptation underlying ethanol dependence.

Finally, we evaluated which of the administered SCFAs is the most potent for reducing chronic ethanol intake. Remarkably, we observed that acetate, propionate and butyrate are all capable of significantly reducing chronic alcohol consumption when administered separately. However, butyrate administration generated the most potent therapeutic effect compared to the other SCFAs, and it did so in a dose–response manner. It is interesting to note that when butyrate is no longer administered, UChB animals quickly recover their characteristic high ethanol intake, indicating that the anti-addictive effect is transient.

Increase evidence suggests that epigenetic modifications, in particular histone acetylation, are key mechanisms by which long-lasting changes on neural gene expression can occur, ultimately explaining the

persistence of alcohol addictive behaviors<sup>73,74</sup>. In the rodent brain, different studies reported epigenetic alterations following ethanol exposure associated with an increase in HDAC expression, leading to alcohol tolerance and dependence<sup>73,74</sup>. Among the SCFAs, butyrate is the most potent in inhibiting HDAC activities, both *in vitro* and *in vivo*<sup>32</sup>, promoting gene expression. In this study, we observed that sodium butyrate administration to chronically alcohol-drinking animals induced a significant increase in the levels of H3-histone acetylation, in both striatum and prefrontal cortex, which are brain areas playing a key roles in mediating the chronic effects of drugs of abuse<sup>38</sup>. These findings indicate that the intragastrical administered sodium butyrate can reach the brain and induce a pharmacological effect, as SCFAs have the ability to penetrate the brain<sup>24</sup>. The hyperacetylation in these brain regions has also been reported after intraperitoneal administration of butyrate<sup>43</sup>. Nevertheless, further studies are needed to fully understand the mechanism behind the therapeutic effects, since SCFAs and butyrate may also directly influence the brain by reinforcing the brain-blood-barrier integrity, increasing tight junction protein expression<sup>75</sup>, modulating neurotransmission and influencing levels of several neurotrophic factors<sup>76–78</sup>, which are reduced after chronic ethanol intake<sup>73</sup>. Additionally, chromatin remodeling and active gene transcription is crucial to the formation of long-term memories in the brain reward circuitry<sup>79,80</sup>. Thus, SCFAs administration, through their HDAC inhibition activity, may play a role in the reduction of the persistence of memories associated with drug use.

## Conclusion

Altogether, this study demonstrated that intragastric administration of SCFAs, and specially butyrate, can prevent the initiation of ethanol intake and to strongly reduce voluntary ethanol intake once chronic alcohol intake is already established. These therapeutics effects were associated with the reduction of ethanol-induced alteration of intestinal architecture, intestinal, liver and brain inflammation, and the increase in histone acetylation levels in striatum and prefrontal cortex. Thus, dietary butyrate supplementation is a highly appealing approach for the treatment of alcohol use disorder, as it represents a simple, inexpensive, and relatively low-risk method to improve the outcomes induced by chronic alcohol abuse. Through more research is needed to validate the effectiveness of this dietary intervention, it remains a promising strategy to be used in the future in conjunction with traditional pharmacological and psychological interventions.

## Methods

### Animals

Two-month-old male Wistar-derived rats, selectively bred for over 90 generations as ethanol consumers (University of Chile Bibulous; UChB)<sup>81</sup>, were used. Animals were housed individually and maintained on a 12-h light/dark cycle and regularly fed a soy protein, peanut-meal rodent diet (Cisternas, Santiago, Chile). All procedures were approved by the Ethics Committee for Experiments with Laboratory Animals at the Medical Faculty of the Universidad de Chile (Protocol CBA# 0994 FMUCH). All methods were performed in accordance with the ARRIVE guidelines, the SAGER guidelines, and with relevant institutional, national, and international guidelines and regulations for the care and use of laboratory animals.

### Drugs

Ethanol solutions were prepared from absolute ethanol (Merck) diluted to 10% in tap water. Sodium acetate, sodium propionate and sodium butyrate (Sigma-Aldrich) were dissolved in distilled water, adjusted to pH 7.2, and administered by oral gavage in a volume of 6 mL/kg/day twice-daily. Previous studies have shown that administering moderate amounts of sodium can increase water consumption<sup>82</sup>. Thus, to rule out the influence of sodium contained in the SCFAs dose on ethanol consumption, an additional control group was generated which received a dose of 554 mg/kg of NaCl, corresponding to the same concentration of sodium (9.5 mmol/kg) as that received by the SCFAs-treated animals.

### Effect of intragastric administration of SCFAs on alcohol intake in naïve animals

To evaluate the role of SCFAs on the acquisition phase of ethanol intake, two-month-old UChB ethanol-naïve animals were divided into three groups ( $n=6$  per experimental group). Animals were treated by oral gavage with either (1) a combination of SCFAs (300 mg/kg each sodium acetate, sodium propionate, and sodium butyrate); (2) 554 mg/kg NaCl solution; or (3) distilled water (vehicle). This SCFA dose was chosen based on previous studies in rats, where potent therapeutic effects, such as a reduction in neuroinflammation and depressive-like behavior, were reported following its administration<sup>83</sup>. Treatments were administered twice-daily for six days before animals were given continuous free-choice access between 10% ethanol solution and tap water, as previously described<sup>5</sup>. SCFAs or vehicle administrations were maintained for an additional seven days. Ethanol and water intake were recorded daily. Ethanol intake was expressed in grams of ethanol consumed per kilogram of body weight per day, while ethanol preference was expressed as a percentage of total fluid intake, calculated as the sum of daily alcohol and water consumption.

### Effect of intragastric administration of SCFAs on alcohol intake in chronically ethanol-consuming animals and sample collection

To evaluate the role of SCFAs in the maintenance phase of ethanol intake, two-month-old ethanol-naïve UChB animals received continuous free-choice access to 10% ethanol solution and water for 58 days. On that day, animals were divided into three groups ( $n=6$  per experimental group) and treated by oral gavage with either (1) a combination of SCFAs (300 mg/kg each sodium acetate, sodium propionate, and sodium butyrate); (2) 554 mg/kg NaCl solution; or (3) distilled water (vehicle). Treatments were administered twice-daily for five days. Free-choice ethanol and water access was maintained during SCFAs and vehicle administrations. Ethanol and

water intake were recorded daily. After the last measuring of ethanol consumption animals were anesthetized with a cocktail of 60 mg/kg ketamine, 10 mg/kg xylazine, and 4 mg/kg acepromazine, and blood samples were obtained by cardiac puncture, and were intracardially perfused with 100 mL of 0.1 M PBS (euthanasia). After perfusion, samples of proximal colon, liver, and brain were obtained and frozen or fixed in 4% paraformaldehyde (Merck). One brain hemisphere was fixed for the analysis of astrocyte and microglia immunoreactivity in the stratum radiatum of the CA1 region of the hippocampus. From the contralateral frozen hemisphere, the nucleus accumbens was used to assess transcriptional dynamics, while the striatum and prefrontal cortex were used to assess histone H3 acetylation levels.

### Histopathological analysis of intestinal architecture

Samples of proximal colon ( $n=6$  per experimental group) were paraffin-embedded, and 4  $\mu\text{m}$ -histological sections were stained with hematoxylin/eosin, and evaluated based on intestinal damage criteria<sup>33</sup> by an experienced pathologist. Crypt length and inflammatory infiltrate were analyzed using QuPath software (v.0.5.1). Crypt length was determined by measuring a straight line from the base of the crypt to the apical surface. Inflammatory infiltrate was determined by counting cell numbers per area in the lamina propria compartment of each sample<sup>33</sup>.

### Immunohistochemistry staining and analysis of proximal colon samples

Paraffin-embedded histological sections (4  $\mu\text{m}$  thick) derived from proximal colon samples obtained from animals of the different experimental groups ( $n=6$  per experimental group), were stained with rabbit polyclonal anti-PCNA antibody (1:300, Novus Biologicals, Cat. NB600-1331) to evaluate the proportion of proliferating cells in colon tissue. Briefly, the sections were subjected to deparaffinization with NeoClear, (Merck) and rehydrated with a battery of alcohols from absolute ethanol to 70% ethanol. Antigen retrieval was performed with sodium citrate buffer (pH 6). Then, IHC was performed with VECTASTAIN® Elite® ABC-HRP Kit, Peroxidase, R.T.U. (Universal) (PK-7200) and DAB substrate from VectorLabs, following the manufacturer instructions.

Positivity Index (pixels per area) was calculated with QuPath software (v.0.5.1), creating a classifier with the following parameters: Moderate resolution (2.01 mm/pixel), DAB channel, smoothing sigma 1, 0.29 threshold. Staining above this threshold index was considered positive and below was identified as negative. We selected lamina propria areas for each sample and mean positivity index from DAB stain was compared among different experimental groups.

### Quantification of mRNA levels of pro-inflammatory factors in the proximal colon and liver

Total RNA was purified from of proximal colon and liver samples ( $n=6$  per experimental group) using Trizol (Invitrogen) and used to perform reverse transcription with MMLV reverse transcriptase (Invitrogen). qPCR reactions were conducted using a QuantStudio 12 K-Flex equipment (Thermo-Fisher) to amplify the mRNA levels of interleukins IL1 $\beta$ , IL6, IL8, TNF- $\alpha$  and lipopolysaccharide binding protein (LBP) using specific primers (Supplementary Table 1). The mRNA level of each target gene was normalized against the mRNA level of  $\beta$ -actin in the same sample.

### Determination of LPS levels in blood samples

LPS levels were determined in plasma samples ( $n=6$  per experimental group) using the LPS enzyme-linked immunosorbent assay (ELISA) kit (MyBiosource) as previously reported<sup>5</sup>.

### Determination of astrocyte and microglia immunoreactivity

Double-labeling immunofluorescence against the astrocyte marker glial fibrillary acidic protein (GFAP) (Sigma-Aldrich G3893; 1:500 dilution) and the microglial marker ionized binding protein1 (Iba1) (Wako 019-19741, 1:400 dilution) was performed on 30  $\mu\text{m}$ -coronal cryosections of one brain hemisphere ( $n=6$  per experimental group). Six microphotographs of the *stratum radiatum* of the CA1 region in the hippocampus per hemisphere were captured using an Olympus FV10i confocal microscope with a 60 $\times$ objective lens (NA 1.30) and FV10-ASW-2b software. Astrocyte surface area, total process length, and the ramification index (ratio of total process length to the number of branch points) were quantified using FIJI software with the Simple Neurite Tracer plugin, according to previous reports<sup>84</sup>. Microglial reactivity, typically involving a shift from a highly ramified to a more compact, amoeboid shape characterized by a larger soma and retracted processes was quantified using the Solidity metric. Solidity is defined as the ratio of total cell area (including soma and processes) to convex cell area (the smallest convex polygon encompassing the entire cell). Higher solidity values indicate a more compact morphology typical of reactive microglia<sup>58,85</sup>.

### Evaluation of transcriptomic dynamics in the nucleus accumbens

The nucleus accumbens of one brain hemisphere was used for RNA purification with the total RNA purification kit (Qiagen). mRNA samples ( $n=4$  per experimental group) were sequenced using TruSeq stranded mRNA library + NovaSeq6000-150PE platform (Macrogen) with 6 million reads per sample. The raw data from RNA-seq libraries were processed, and reads of low quality were filtered out with Trimmomatic software (v0.39)<sup>86</sup>. The clean reads were mapped to the rat reference genome (Rattus\_norvegicus.mRatBN7.2) with HISAT2 software (v2.2.1)<sup>87</sup>, and quantified with featureCounts software (V2.0.1)<sup>88</sup>. The differential expression analysis was performed using pyDESeq2 software (v0.4.4)<sup>89</sup>. Differentially expressed genes (DEGs) were determined based on the criteria of  $p.\text{adj} < 0.05$  and  $\log_2 \text{fold change (FC)} > 0.58$ , selecting genes with a change in expression of at least 50%. The gene ontology analysis (GO) was performed with the DAVID (v2024q1) database<sup>90</sup>. The RNA sequencing data have been deposited in the Genome Sequence Archive (GSA) under the accession number PRJCA032120.

### Comparison of the potency of the three SCFAs to inhibit ethanol consumption

Two-month-old UChB ethanol-naïve animals received continuous free-choice access to 10% ethanol solution and water for 44 days. On that day, animals were divided into five groups ( $n=6$  per experimental group) and treated by oral gavage with either (1) a combination of SCFAs (300 mg/kg each sodium acetate, sodium propionate, and sodium butyrate); (2) 300 mg/kg sodium acetate; (3) 300 mg/kg sodium propionate; (4) 300 mg/kg sodium butyrate; or (5) distilled water. Treatments were administered twice-daily for five days. Free-choice ethanol and water access was maintained during treatment administration. Ethanol and water intake were recorded daily.

### Dose-response determination of sodium butyrate in reducing alcohol intake in chronically ethanol-consuming animals

Two-month-old UChB ethanol-naïve animals received continuous free-choice access to 10% ethanol solution and water for 64 days. On that day, animals were divided into groups ( $n=6$  per experimental group) and treated by oral gavage with either (1) 300 mg/kg sodium butyrate; (2) 30 mg/kg sodium butyrate; (3) 3 mg/kg sodium butyrate; or (4) distilled water. Treatments were administered twice-daily for five days. Free-choice ethanol and water access was maintained during treatment administration and then continued for six additional days after treatments discontinuation to assess the duration of the effects. Ethanol and water intake were recorded daily.

### Evaluation of H3 histone acetylation levels in the striatum and prefrontal cortex

Twenty-four hours after the last administration of 300 mg/kg sodium butyrate or vehicle, animals were anesthetized with a cocktail of 60 mg/kg ketamine, 10 mg/kg xylazine, and 4 mg/kg acepromazine, and were intracardially perfused with 100 mL of 0.1 M PBS (euthanasia). Then, striatum and prefrontal cortex of one brain hemisphere were dissected and frozen ( $n=6$  per experimental group). Total proteins were extracted using a T-per lysis buffer (Thermo-Fisher). For Western Blots, 25 µg of proteins was utilized to assess striatal and prefrontal cortex levels of H3 histone acetylation (AcH3) with an anti-AcH3 primary antibody (Thermo, MA5-11195, 1:500 dilution). Histone H4 and β-actin were used as loading controls. Histone H4 was detected with an anti-H4 primary antibody (Cell Signaling, 13,919, 1:500 dilution), while β-actin was evaluated with an anti-β-actin primary antibody (Santa Cruz Biotechnology, sc-47778, 1:2000 dilution). Detection of reactive bands was performed using the Odyssey Imagen System (Li-COR) as previously reported<sup>91</sup>.

### Statistical analyses

Data are expressed as mean  $\pm$  SEM. Statistical analyses were performed using GraphPad Prism v.9.2.0 software. The normal distribution of data for all experiments was evaluated using the Shapiro-Wilk test. For normally distributed data, one-way ANOVA or two-way ANOVA was used followed by Bonferroni or Tukey post-hoc test. A level of  $p < 0.05$  was considered for statistical significance.

### Data availability

Data generated during this study are included in this published article and its supplementary information files. Additionally, the RNA sequencing data have been deposited in the Genome Sequence Archive (GSA) under the accession number PRJCA032120.

Received: 28 August 2024; Accepted: 18 November 2024

Published online: 26 November 2024

### References

- Peacock, A. et al. Global statistics on alcohol, tobacco and illicit drug use: 2017 status report. *Addiction* **113**, 1905–1926. <https://doi.org/10.1111/add.14234> (2018).
- Gilpin, N. W. & Koob, G. F. Neurobiology of alcohol dependence: focus on motivational mechanisms. *Alcohol Res. Health* **31**, 185–195 (2008).
- Johnson, B. A. Update on neuropharmacological treatments for alcoholism: Scientific basis and clinical findings. *Biochem. Pharmacol.* **75**, 34–56. <https://doi.org/10.1016/j.bcp.2007.08.005> (2008).
- Round, J. L. & Mazmanian, S. K. The gut microbiota shapes intestinal immune responses during health and disease. *Nat. Rev. Immunol.* **9**, 313–323. <https://doi.org/10.1038/nri2515> (2009).
- Ezquer, F. et al. Innate gut microbiota predisposes to high alcohol consumption. *Addict. Biol.* **26**, e13018. <https://doi.org/10.1111/adb.13018> (2021).
- Lucerne, K. E. & Kiraly, D. D. The role of gut-immune-brain signaling in substance use disorders. *Int. Rev. Neurobiol.* **157**, 311–370. <https://doi.org/10.1016/bs.irn.2020.09.005> (2021).
- Bjorkhaug, S. T. et al. Characterization of gut microbiota composition and functions in patients with chronic alcohol overconsumption. *Gut Microbes* **10**, 663–675. <https://doi.org/10.1080/19490976.2019.1580097> (2019).
- Leclercq, S., de Timaré, P., Delzenne, N. M. & Starkel, P. The link between inflammation, bugs, the intestine and the brain in alcohol dependence. *Transl. Psychiatry* **7**, e1048. <https://doi.org/10.1038/tp.2017.15> (2017).
- Ezquer, F. et al. A dual treatment blocks alcohol binge-drinking relapse: Microbiota as a new player. *Drug Alcohol Depend.* **236**, 109466. <https://doi.org/10.1016/j.drugdep.2022.109466> (2022).
- Bull-Otterson, L. et al. Metagenomic analyses of alcohol induced pathogenic alterations in the intestinal microbiome and the effect of *Lactobacillus rhamnosus* GG treatment. *PLoS One* **8**, e53028. <https://doi.org/10.1371/journal.pone.0053028> (2013).
- Garcia-Cabrerizo, R., Carbia, C., Kj, O. R., Schellekens, H. & Cryan, J. F. Microbiota-gut-brain axis as a regulator of reward processes. *J. Neurochem.* **157**, 1495–1524. <https://doi.org/10.1111/jnc.15284> (2021).
- Keshavarzian, A. et al. Evidence that chronic alcohol exposure promotes intestinal oxidative stress, intestinal hyperpermeability and endotoxemia prior to development of alcoholic steatohepatitis in rats. *J. Hepatol.* **50**, 538–547. <https://doi.org/10.1016/j.jhep.2008.10.028> (2009).
- Forsyth, C. B. et al. Lactobacillus GG treatment ameliorates alcohol-induced intestinal oxidative stress, gut leakiness, and liver injury in a rat model of alcoholic steatohepatitis. *Alcohol* **43**, 163–172. <https://doi.org/10.1016/j.alcohol.2008.12.009> (2009).
- Leclercq, S. et al. Role of intestinal permeability and inflammation in the biological and behavioral control of alcohol-dependent subjects. *Brain Behav. Immun.* **26**, 911–918. <https://doi.org/10.1016/j.bbi.2012.04.001> (2012).

15. Leclercq, S. et al. Intestinal permeability, gut-bacterial dysbiosis, and behavioral markers of alcohol-dependence severity. *Proc. Natl. Acad. Sci. U. S. A.* **111**, E4485–4493. <https://doi.org/10.1073/pnas.1415174111> (2014).
16. Valles, S. L., Blanco, A. M., Pascual, M. & Guerri, C. Chronic ethanol treatment enhances inflammatory mediators and cell death in the brain and in astrocytes. *Brain Pathol.* **14**, 365–371. <https://doi.org/10.1111/j.1750-3639.2004.tb00079.x> (2004).
17. Kaminska, B., Mota, M. & Pizzi, M. Signal transduction and epigenetic mechanisms in the control of microglia activation during neuroinflammation. *Biochim. Biophys. Acta* **339–351**, 2016. <https://doi.org/10.1016/j.bbadi.2015.10.026> (1862).
18. Wu, T., Cai, W. & Chen, X. Epigenetic regulation of neurotransmitter signaling in neurological disorders. *Neurobiol. Dis.* **184**, 106232. <https://doi.org/10.1016/j.nbd.2023.106232> (2023).
19. Crews, F. T., Zou, J. & Qin, L. Induction of innate immune genes in brain create the neurobiology of addiction. *Brain Behav. Immun.* **25**(Suppl 1), S4–S12. <https://doi.org/10.1016/j.bbi.2011.03.003> (2011).
20. Ward, R. J. et al. Neuro-inflammation induced in the hippocampus of ‘binge drinking’ rats may be mediated by elevated extracellular glutamate content. *J. Neurochem.* **111**, 1119–1128. <https://doi.org/10.1111/j.1471-4159.2009.06389.x> (2009).
21. Alfonso-Lloches, S., Pascual-Lucas, M., Blanco, A. M., Sanchez-Vera, I. & Guerri, C. Pivotal role of TLR4 receptors in alcohol-induced neuroinflammation and brain damage. *J. Neurosci.* **30**, 8285–8295. <https://doi.org/10.1523/JNEUROSCI.0976-10.2010> (2010).
22. Blednov, Y. A. et al. Activation of inflammatory signaling by lipopolysaccharide produces a prolonged increase of voluntary alcohol intake in mice. *Brain Behav. Immun.* **25**(Suppl 1), S92–S105. <https://doi.org/10.1016/j.bbi.2011.01.008> (2011).
23. Vatsalya, V. et al. The beneficial effects of lactobacillus GG therapy on liver and drinking assessments in patients with moderate alcohol-associated hepatitis. *Am. J. Gastroenterol.* **118**, 1457–1460. <https://doi.org/10.14309/ajg.0000000000002283> (2023).
24. Silva, Y. P., Bernardi, A. & Frozza, R. L. The role of short-chain fatty acids from gut microbiota in gut-brain communication. *Front. Endocrinol. (Lausanne)* **11**, 25. <https://doi.org/10.3389/fendo.2020.00025> (2020).
25. Russo, I., Luciani, A., De Cicco, P., Troncone, E. & Ciacci, C. Butyrate attenuates lipopolysaccharide-induced inflammation in intestinal cells and Crohn’s mucosa through modulation of antioxidant Defense machinery. *PLoS One* **7**, e32841. <https://doi.org/10.1371/journal.pone.0032841> (2012).
26. Salvi, P. S. & Cowles, R. A. Butyrate and the intestinal epithelium: Modulation of proliferation and inflammation in homeostasis and disease. *Cells* **10**. <https://doi.org/10.3390/cells10071775> (2021).
27. Stilling, R. M. et al. The neuropharmacology of butyrate: The bread and butter of the microbiota-gut-brain axis?. *Neurochem. Int.* **99**, 110–132. <https://doi.org/10.1016/j.neuint.2016.06.011> (2016).
28. MacFabe, D. F., Cain, N. E., Boon, F., Ossenkopp, K. P. & Cain, D. P. Effects of the enteric bacterial metabolic product propionic acid on object-directed behavior, social behavior, cognition, and neuroinflammation in adolescent rats: Relevance to autism spectrum disorder. *Behav. Brain Res.* **217**, 47–54. <https://doi.org/10.1016/j.bbr.2010.10.005> (2011).
29. Govindarajan, N., Agis-Balboa, R. C., Walter, J., Sananbenesi, F. & Fischer, A. Sodium butyrate improves memory function in an Alzheimer’s disease mouse model when administered at an advanced stage of disease progression. *J. Alzheimers Dis.* **26**, 187–197. <https://doi.org/10.3233/JAD-2011-110080> (2011).
30. Patnala, R., Arumugam, T. V., Gupta, N. & Dheen, S. T. HDAC inhibitor sodium butyrate-mediated epigenetic regulation enhances neuroprotective function of microglia during Ischemic stroke. *Mol. Neurobiol.* **54**, 6391–6411. <https://doi.org/10.1007/s12035-016-0149-z> (2017).
31. Mostafa, H. et al. Plasma metabolic biomarkers for discriminating individuals with alcohol use disorders from social drinkers and alcohol-naïve subjects. *J. Subst. Abuse Treat.* **77**, 1–5. <https://doi.org/10.1016/j.jsat.2017.02.015> (2017).
32. Liu, H. et al. Butyrate: A double-edged sword for health?. *Adv. Nutr.* **9**, 21–29. <https://doi.org/10.1093/advances/nmx009> (2018).
33. Li, T. T. et al. Glutamate microinjection into the hypothalamic paraventricular nucleus attenuates ulcerative colitis in rats. *Acta Pharmacol. Sin.* **35**, 185–194. <https://doi.org/10.1038/aps.2013.140> (2014).
34. D’Antongiovanni, V. et al. Pathological remodeling of the gut barrier as a prodromal event of high-fat diet-induced obesity. *Lab. Invest.* **103**, 100194. <https://doi.org/10.1016/j.labinv.2023.100194> (2023).
35. Quintanilla, M. E. et al. Intranasal mesenchymal stem cell secretome administration markedly inhibits alcohol and nicotine self-administration and blocks relapse-intake: Mechanism and translational options. *Stem Cell Res. Ther.* **10**, 205. <https://doi.org/10.1186/s13287-019-1304-z> (2019).
36. Walter, N. et al. Effect of chronic ethanol consumption in rhesus macaques on the nucleus accumbens core transcriptome. *Addict. Biol.* **26**, e13021. <https://doi.org/10.1111/adb.13021> (2021).
37. Davie, J. R. Inhibition of histone deacetylase activity by butyrate. *J. Nutr.* **133**, 2485S–2493S. <https://doi.org/10.1093/jn/jn32485S> (2003).
38. Lobo, M. K. & Nestler, E. J. The striatal balancing act in drug addiction: Distinct roles of direct and indirect pathway medium spiny neurons. *Front. Neuroanat.* **5**, 41. <https://doi.org/10.3389/fnana.2011.00041> (2011).
39. Wei, H. et al. Butyrate ameliorates chronic alcoholic central nervous damage by suppressing microglia-mediated neuroinflammation and modulating the microbiome-gut-brain axis. *Biomed. Pharmacother.* **160**, 114308. <https://doi.org/10.1016/j.bioph.2023.114308> (2023).
40. Cryan, J. F. & Dinan, T. G. Mind-altering microorganisms: the impact of the gut microbiota on brain and behaviour. *Nat. Rev. Neurosci.* **13**, 701–712. <https://doi.org/10.1038/nrn3346> (2012).
41. Reyes, R. E. N., Al Omran, A. J., Davies, D. L. & Asatryan, L. Antibiotic-induced disruption of commensal microbiome linked to increases in binge-like ethanol consumption behavior. *Brain Res.* **1747**, 147067. <https://doi.org/10.1016/j.brainres.2020.147067> (2020).
42. Reyes, R. E., Gao, L., Zhang, Z., Davies, D. L. & Asatryan, L. Supplementation with sodium butyrate protects against antibiotic-induced increases in ethanol consumption behavior in mice. *Alcohol* **100**, 1–9. <https://doi.org/10.1016/j.alcohol.2021.12.003> (2022).
43. Simon-O’Brien, E. et al. The histone deacetylase inhibitor sodium butyrate decreases excessive ethanol intake in dependent animals. *Addict. Biol.* **20**, 676–689. <https://doi.org/10.1111/adb.12161> (2015).
44. Hofford, R. S. et al. Alterations in microbiome composition and metabolic byproducts drive behavioral and transcriptional responses to morphine. *Neuropsychopharmacology* **46**, 2062–2072. <https://doi.org/10.1038/s41386-021-01043-0> (2021).
45. Meckel, K. R. et al. Microbial short-chain fatty acids regulate drug seeking and transcriptional control in a model of cocaine seeking. *Neuropsychopharmacology* **49**, 386–395. <https://doi.org/10.1038/s41386-023-01661-w> (2024).
46. Ron, D. & Barak, S. Molecular mechanisms underlying alcohol-drinking behaviours. *Nat. Rev. Neurosci.* **17**, 576–591. <https://doi.org/10.1038/nrn.2016.85> (2016).
47. Al-Sadi, R., Boivin, M. & Ma, T. Mechanism of cytokine modulation of epithelial tight junction barrier. *Front. Biosci. (Landmark Ed)* **14**, 2765–2778. <https://doi.org/10.2741/3413> (2009).
48. Chen, P., Starkel, P., Turner, J. R., Ho, S. B. & Schnabl, B. Dysbiosis-induced intestinal inflammation activates tumor necrosis factor receptor I and mediates alcoholic liver disease in mice. *Hepatology* **61**, 883–894. <https://doi.org/10.1002/hep.27489> (2015).
49. Mowat, A. M. & Agace, W. W. Regional specialization within the intestinal immune system. *Nat. Rev. Immunol.* **14**, 667–685. <https://doi.org/10.1038/nri3738> (2014).
50. Venkatraman, A. et al. Amelioration of dextran sulfate colitis by butyrate: Role of heat shock protein 70 and NF-kappaB. *Am. J. Physiol. Gastrointest. Liver Physiol.* **285**, G177–184. <https://doi.org/10.1152/ajpgi.00307.2002> (2003).
51. Mayfield, J., Ferguson, L. & Harris, R. A. Neuroimmune signaling: A key component of alcohol abuse. *Curr. Opin. Neurobiol.* **23**, 513–520. <https://doi.org/10.1016/j.conb.2013.01.024> (2013).

52. Zhang, T. et al. Butyrate ameliorates alcoholic fatty liver disease via reducing endotoxemia and inhibiting liver gasdermin D-mediated pyroptosis. *Ann. Transl. Med.* **9**, 873. <https://doi.org/10.21037/atm-21-2158> (2021).
53. Elamin, E. E., Masclee, A. A., Dekker, J., Pieters, H. J. & Jonkers, D. M. Short-chain fatty acids activate AMP-activated protein kinase and ameliorate ethanol-induced intestinal barrier dysfunction in Caco-2 cell monolayers. *J. Nutr.* **143**, 1872–1881. <https://doi.org/10.3945/jn.113.179549> (2013).
54. Ma, X. et al. Butyrate promotes the recovering of intestinal wound healing through its positive effect on the tight junctions. *J. Anim. Sci.* **90**(Suppl 4), 266–268. <https://doi.org/10.2527/jas.50965> (2012).
55. Xia, Z. et al. Oral administration of propionic acid during lactation enhances the colonic barrier function. *Lipids Health Dis.* **16**, 62. <https://doi.org/10.1186/s12944-017-0452-3> (2017).
56. Parada Venegas, D. et al. Short chain fatty acids (SCFAs)-mediated gut epithelial and immune regulation and its relevance for inflammatory bowel diseases. *Front. Immunol.* **10**, 277. <https://doi.org/10.3389/fimmu.2019.00277> (2019).
57. Norden, D. M., Trojanowski, P. J., Villanueva, E., Navarro, E. & Godbout, J. P. Sequential activation of microglia and astrocyte cytokine expression precedes increased Iba-1 or GFAP immunoreactivity following systemic immune challenge. *Glia* **64**, 300–316. <https://doi.org/10.1002/glia.22930> (2016).
58. Martinez, A. et al. Characterization of microglia behaviour in healthy and pathological conditions with image analysis tools. *Open Biol.* **13**, 220200. <https://doi.org/10.1098/rsob.220200> (2023).
59. Anand, S. K., Ahmad, M. H., Sahu, M. R., Subba, R. & Mondal, A. C. Detrimental effects of alcohol-induced inflammation on brain health: From neurogenesis to neurodegeneration. *Cell Mol. Neurobiol.* **43**, 1885–1904. <https://doi.org/10.1007/s10571-022-01308-2> (2023).
60. Sullivan, E. V., Marsh, L., Mathalon, D. H., Lim, K. O. & Pfefferbaum, A. Anterior hippocampal volume deficits in nonamnesic, aging chronic alcoholics. *Alcohol Clin. Exp. Res.* **19**, 110–122. <https://doi.org/10.1111/j.1530-0277.1995.tb01478.x> (1995).
61. Franke, H., Kittner, H., Berger, P., Wirkner, K. & Schramek, J. The reaction of astrocytes and neurons in the hippocampus of adult rats during chronic ethanol treatment and correlations to behavioral impairments. *Alcohol* **14**, 445–454. [https://doi.org/10.1016/s0741-8329\(96\)00209-1](https://doi.org/10.1016/s0741-8329(96)00209-1) (1997).
62. Berrios-Carcamo, P. et al. Oxidative stress and neuroinflammation as a pivot in drug abuse. A focus on the therapeutic potential of antioxidant and anti-inflammatory agents and biomolecules. *Antioxidants (Basel)* **9**. <https://doi.org/10.3390/antiox9090830> (2020).
63. Ezquer, F. et al. Intranasal delivery of mesenchymal stem cell-derived exosomes reduces oxidative stress and markedly inhibits ethanol consumption and post-deprivation relapse drinking. *Addict. Biol.* **24**, 994–1007. <https://doi.org/10.1111/adb.12675> (2019).
64. Crews, F. T. Alcohol-related neurodegeneration and recovery: mechanisms from animal models. *Alcohol Res. Health* **31**, 377–388 (2008).
65. Hermens, D. F. et al. Hippocampal glutamate is increased and associated with risky drinking in young adults with major depression. *J. Affect. Disord.* **186**, 95–98. <https://doi.org/10.1016/j.jad.2015.07.009> (2015).
66. Bachmann, C., Colombo, J. P. & Beruter, J. Short chain fatty acids in plasma and brain: Quantitative determination by gas chromatography. *Clin. Chim. Acta* **92**, 153–159. [https://doi.org/10.1016/0009-8981\(79\)90109-8](https://doi.org/10.1016/0009-8981(79)90109-8) (1979).
67. Liu, J. et al. Neuroprotective effects of clostridium butyricum against vascular dementia in mice via metabolic butyrate. *Biomed. Res. Int.* **2015**, 412946. <https://doi.org/10.1155/2015/412946> (2015).
68. McClain, J. A. et al. Adolescent binge alcohol exposure induces long-lasting partial activation of microglia. *Brain Behav. Immun.* **25**(Suppl 1), S120–128. <https://doi.org/10.1016/j.bbi.2011.01.006> (2011).
69. Gao, L., Davies, D. L. & Asatryan, L. Sodium butyrate supplementation modulates neuroinflammatory response aggravated by antibiotic treatment in a mouse model of binge-like ethanol drinking. *Int J Mol Sci* **23**. <https://doi.org/10.3390/ijms232415688> (2022).
70. Fu, S. P. et al. Anti-inflammatory effects of BHBA in both in vivo and in vitro Parkinson's disease models are mediated by GPR109A-dependent mechanisms. *J. Neuroinflammation* **12**, 9. <https://doi.org/10.1186/s12974-014-0230-3> (2015).
71. Salgado, S. & Kaplitt, M. G. The nucleus accumbens: A comprehensive review. *Stereotact. Funct. Neurosurg.* **93**, 75–93. <https://doi.org/10.1159/000368279> (2015).
72. Kapoor, M. et al. Analysis of whole genome-transcriptomic organization in brain to identify genes associated with alcoholism. *Transl. Psychiatry* **9**, 89. <https://doi.org/10.1038/s41398-019-0384-y> (2019).
73. Pascual, M. et al. Changes in histone acetylation in the prefrontal cortex of ethanol-exposed adolescent rats are associated with ethanol-induced place conditioning. *Neuropharmacology* **62**, 2309–2319. <https://doi.org/10.1016/j.neuropharm.2012.01.011> (2012).
74. Starkman, B. G., Sakharkar, A. J. & Pandey, S. C. Epigenetics-beyond the genome in alcoholism. *Alcohol Res.* **34**, 293–305 (2012).
75. Braniste, V. et al. The gut microbiota influences blood-brain barrier permeability in mice. *Sci. Transl. Med.* **6**, 263ra158. <https://doi.org/10.1126/scitranslmed.3009759> (2014).
76. Wei, Y., Melas, P. A., Wegener, G., Mathe, A. A. & Lavebratt, C. Antidepressant-like effect of sodium butyrate is associated with an increase in TET1 and in 5-hydroxymethylation levels in the Bdnf gene. *Int. J. Neuropsychopharmacol.* **18**. <https://doi.org/10.1093/ijnp/pyu032> (2014).
77. Barichello, T. et al. Sodium butyrate prevents memory impairment by re-establishing BDNF and GDNF expression in experimental pneumococcal meningitis. *Mol. Neurobiol.* **52**, 734–740. <https://doi.org/10.1007/s12035-014-8914-3> (2015).
78. Valvassori, S. S. et al. Sodium butyrate functions as an antidepressant and improves cognition with enhanced neurotrophic expression in models of maternal deprivation and chronic mild stress. *Curr. Neurovasc. Res.* **11**, 359–366. <https://doi.org/10.2174/156720261166140829162158> (2014).
79. Alberini, C. M. Transcription factors in long-term memory and synaptic plasticity. *Physiol. Rev.* **89**, 121–145. <https://doi.org/10.1152/physrev.00017.2008> (2009).
80. Kumar, A. et al. Chromatin remodeling is a key mechanism underlying cocaine-induced plasticity in striatum. *Neuron* **48**, 303–314. <https://doi.org/10.1016/j.neuron.2005.09.023> (2005).
81. Israel, Y. et al. Acquisition, maintenance and relapse-like alcohol drinking: Lessons from the UChB rat line. *Front. Behav. Neurosci.* **11**, 57. <https://doi.org/10.3389/fnbeh.2017.00057> (2017).
82. Stricker, E. M., Hoffmann, M. L., Riccardi, C. J. & Smith, J. C. Increased water intake by rats maintained on high NaCl diet: Analysis of ingestive behavior. *Physiol. Behav.* **79**, 621–631. [https://doi.org/10.1016/s0031-9384\(03\)00172-0](https://doi.org/10.1016/s0031-9384(03)00172-0) (2003).
83. Song, L. et al. *Roseburia hominis* alleviates neuroinflammation via short-chain fatty acids through histone deacetylase inhibition. *Mol. Nutr. Food Res.* **66**, e2200164. <https://doi.org/10.1002/mnfr.202200164> (2022).
84. Ezquer, F. et al. Activated mesenchymal stem cell administration inhibits chronic alcohol drinking and suppresses relapse-like drinking in high-alcohol drinker rats. *Addict. Biol.* **24**, 17–27. <https://doi.org/10.1111/adb.12572> (2019).
85. De Felice, E. et al. Microglial diversity along the hippocampal longitudinal axis impacts synaptic plasticity in adult male mice under homeostatic conditions. *J. Neuroinflammation* **19**, 292. <https://doi.org/10.1186/s12974-022-02655-z> (2022).
86. Bolger, A. M., Lohse, M. & Usadel, B. Trimmomatic: A flexible trimmer for Illumina sequence data. *Bioinformatics* **30**, 2114–2120. <https://doi.org/10.1093/bioinformatics/btu170> (2014).
87. Kim, D., Langmead, B. & Salzberg, S. L. HISAT: A fast spliced aligner with low memory requirements. *Nat. Methods* **12**, 357–360. <https://doi.org/10.1038/nmeth.3317> (2015).
88. Liao, Y., Smyth, G. K. & Shi, W. featureCounts: An efficient general purpose program for assigning sequence reads to genomic features. *Bioinformatics* **30**, 923–930. <https://doi.org/10.1093/bioinformatics/btt656> (2014).

89. Love, M. I., Huber, W. & Anders, S. Moderated estimation of fold change and dispersion for RNA-seq data with DESeq2. *Genome Biol.* **15**, 550. <https://doi.org/10.1186/s13059-014-0550-8> (2014).
90. Sherman, B. T. et al. DAVID: a web server for functional enrichment analysis and functional annotation of gene lists (2021 update). *Nucleic Acids Res.* **50**, W216–W221. <https://doi.org/10.1093/nar/gkac194> (2022).
91. Quintanilla, M. E. et al. Chronic voluntary morphine intake is associated with changes in brain structures involved in drug dependence in a rat model of polydrug use. *Int. J. Mol. Sci.* **24**. <https://doi.org/10.3390/ijms242317081> (2023).

## Acknowledgements

This work was supported by FONDECYT 1,240,162 grant to Fernando Ezquer; ACT210012 grant to Fernando Ezquer, David Ramirez and Paola Morales; FONDECYT 1,231,443 grant to Mario Herrera-Marschitz; FONDECYT 1,220,656 grant to David Ramírez; FONDECYT 11,230,904 grant to Glauben Landskron, FONDECYT 11,240,470 to Pablo Berriós-Cárcamo and FONDECYT 1,220,702 grant to Marcela Hermoso. Additional support was provided by FONDEQUIP EQM190110 (QuantStudio 12 K Flex Real-Time PCR System). The technical assistance of Ms. Carmen Almeyda and Mr. Juan Santibañez is greatly appreciated.

## Author contributions

MEQ: Conceptualization, methodology, data obtention and analysis, data curation, final approval of the manuscript; DS: Methodology, data obtention and analysis, data curation, final approval of the manuscript; ED: Data obtention and analysis, data curation, final approval of the manuscript; IVM: Methodology, data obtention and analysis, data curation, final approval of the manuscript; NM: Methodology, data obtention and analysis, data curation, final approval of the manuscript; GL: Methodology, data obtention and analysis, final approval of the manuscript; AD: Methodology, data obtention and analysis, final approval of the manuscript; PM: Methodology, data obtention and analysis, founding acquisition, final approval of the manuscript; DR: Data obtention and analysis, founding acquisition, final approval of the manuscript; MH: Data obtention and analysis, founding acquisition, final approval of the manuscript; BO: Data obtention and analysis, final approval of the manuscript; PBC: Data obtention and analysis, final approval of the manuscript; ME: Data obtention and analysis, final approval of the manuscript; MHM: Data obtention and analysis, founding acquisition, final approval of the manuscript; YI: Conceptualization, writing original draft, final approval of the manuscript; FE: Conceptualization, methodology, data obtention and analysis, founding acquisition, writing original draft, final approval of the manuscript.

## Declarations

### Competing interests

The authors declare no competing interests.

### Additional information

**Supplementary Information** The online version contains supplementary material available at <https://doi.org/10.1038/s41598-024-80228-1>.

**Correspondence** and requests for materials should be addressed to F.E.

**Reprints and permissions information** is available at [www.nature.com/reprints](http://www.nature.com/reprints).

**Publisher's note** Springer Nature remains neutral with regard to jurisdictional claims in published maps and institutional affiliations.

**Open Access** This article is licensed under a Creative Commons Attribution-NonCommercial-NoDerivatives 4.0 International License, which permits any non-commercial use, sharing, distribution and reproduction in any medium or format, as long as you give appropriate credit to the original author(s) and the source, provide a link to the Creative Commons licence, and indicate if you modified the licensed material. You do not have permission under this licence to share adapted material derived from this article or parts of it. The images or other third party material in this article are included in the article's Creative Commons licence, unless indicated otherwise in a credit line to the material. If material is not included in the article's Creative Commons licence and your intended use is not permitted by statutory regulation or exceeds the permitted use, you will need to obtain permission directly from the copyright holder. To view a copy of this licence, visit <http://creativecommons.org/licenses/by-nc-nd/4.0/>.

© The Author(s) 2024